

Supporting Information

Facile Luminescent Tuning of Zn^{II}/Hg^{II} Complexes Based on Flexible, Semi-Rigid and Rigid Polydentate Schiff Base towards from Blue, Green to Red: Structural, Photophysics, Electrochemistry and Theoretical Calculations Studies

Xin-Ming Wang,[†] Shuo Chen,[†] Rui-Qing Fan,^{*,†} Fu-Qiang Zhang,[‡] and Yu-Lin Yang^{*,†}

[†] Department of Chemistry, Harbin Institute of Technology, Harbin 150001, P. R. of China

[‡] Department of Chemistry, Shangqiu Normal University, Shangqiu 476000, P. R. of China

	Content	Page No.
Fig. S1–S3	Infrared spectra of free ligands L¹–L⁶ , and complex 1a–6a, 1b–6b recorded from the KBr pellet	1–3
Fig. S4–S9	¹ H NMR spectra of free ligands L¹–L⁶ and complex 1a–6a, 1b–6b	5–10
Fig. S10	The asymmetric unit of 1b	15
Fig. S11	The coordinating polyhedron of 1a	16
Fig. S12	The 2D supramolecular structure of L⁵	17
Fig. S13	The 2D supramolecular structure of L⁶	17
Fig. S14	UV-Vis absorption spectra of 1b–6b	21
Fig. S15–S17	CH ₂ Cl ₂ solution excitation spectra of free ligands L¹–L⁶ at 298 K	21–22
Fig. S18	Emission spectrum of complexes 1b–6b at 298 K in CH ₂ Cl ₂ solution.	23
Fig. S19	The luminescence decay curves of Schiff base ligands L¹–L⁶ and complexes 1a–6a and 1b–6b in CH ₂ Cl ₂ at 298 K.	24
Fig. S20	Solid state emission spectra of free ligands L¹–L⁶ at 298 K	25
Fig. S21	The luminescence decay curves of Schiff base ligands L¹–L⁶ and complexes 1a–6a and 1b–6b in solid state at 298 K	26
Fig. S22–S28	Error bars for the values of emission lifetimes and quantum efficiency	27–30
Fig. S29	Cyclic voltammograms compounds L⁵, 1a to 1b in CH ₂ Cl ₂ solution.	31
Fig. S30	The plot of <i>I</i> (a,c) vs square root of scan rate	32

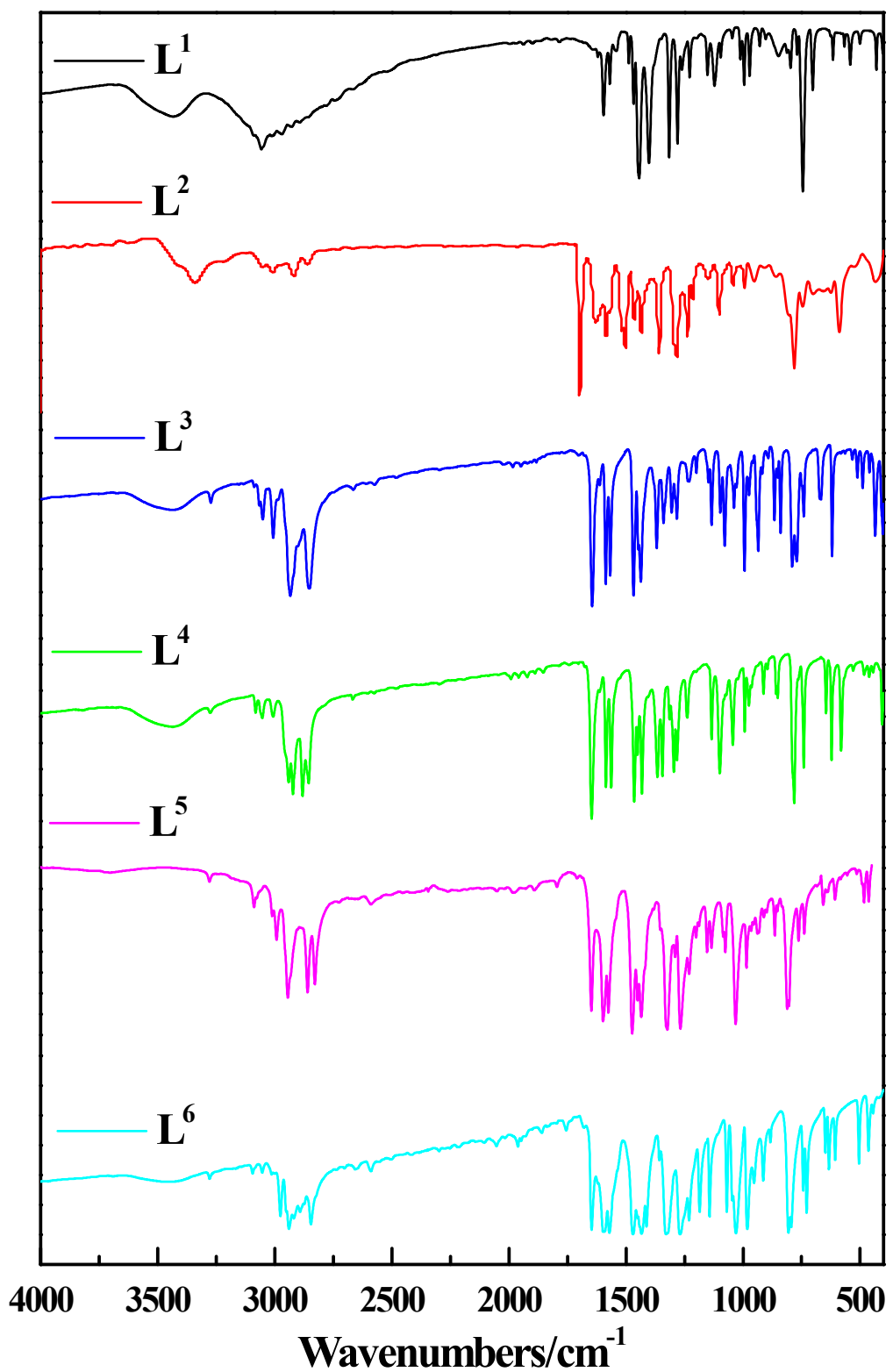


Fig. S1 Infrared spectra of free ligands L^1 – L^6 recorded from a KBr pellet.

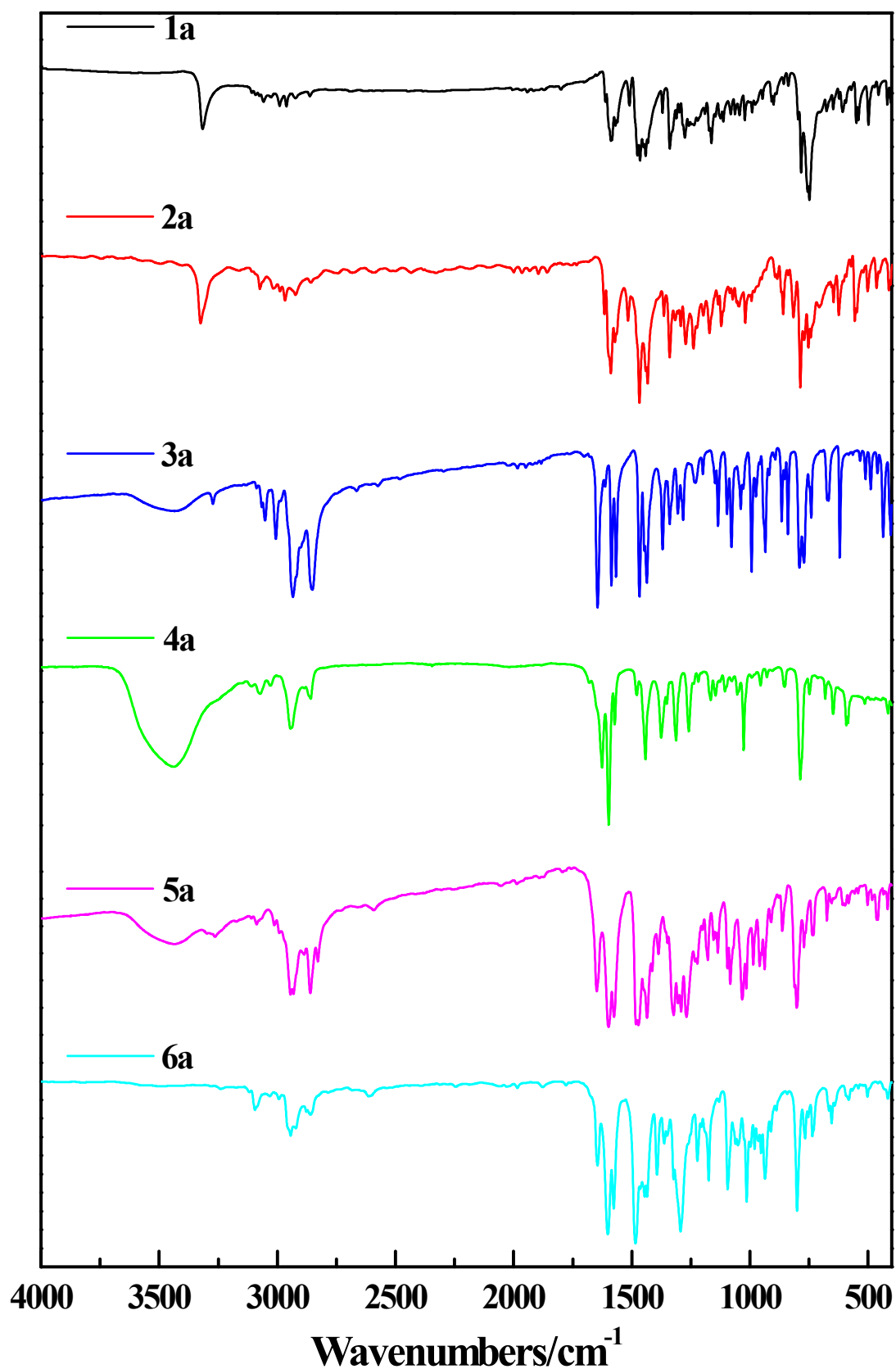


Fig. S2 Infrared spectra of complexes **1a–6a** recorded from a KBr pellet.

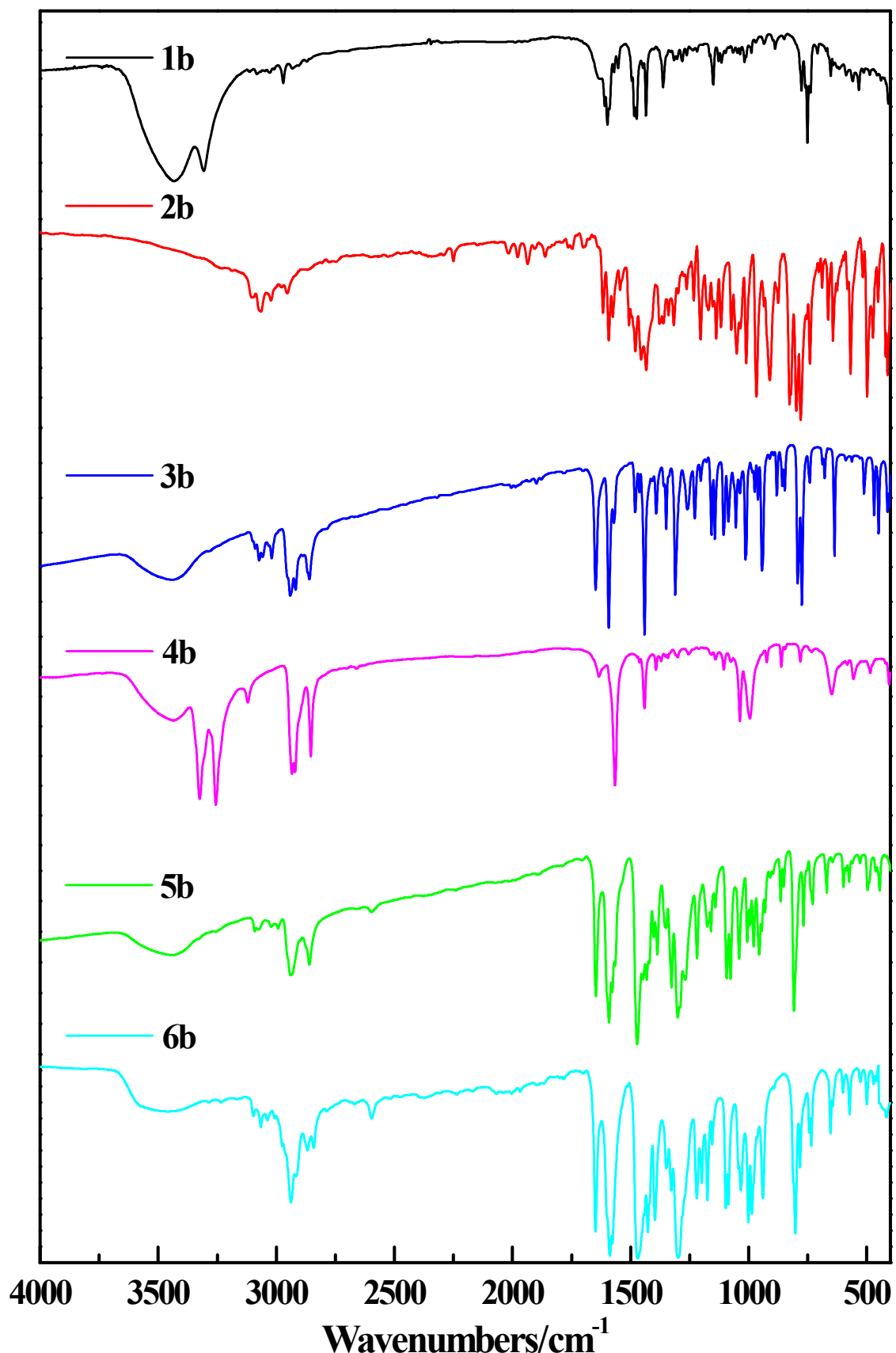


Fig. S3 Infrared spectra of complexes **1b–6b** recorded from a KBr pellet.

IR characteristics

The infrared spectra of ligands (**L¹–L⁶**) and complexes (**1a–6a** and **1b–6b**) were shown in the **Figures S1–S3**. In the spectra of the complexes, the characteristic in-plane and out-of-plane deformation bands of the 2-substituted pyridine rings shift to higher frequencies [*ca.* 30 cm⁻¹ δ (Py) and 20 cm⁻¹ γ (Py)] in comparison with similar free ligands [1103–1154 cm⁻¹ δ (Py) and 880–977 cm⁻¹ γ (Py)], which indicates coordination of pyridine nitrogen atoms.¹ Several bands in the range 2800–3000 cm⁻¹ are assigned to the pyridine ν_{C-H} stretching vibration. The characteristic stretching frequency of the imine “C=N” of the Schiff base moiety at 1653–1601 cm⁻¹ is shifted to a lower wavenumber (1647–1590 cm⁻¹) for complexes. This slight shift signifies the coordination through the nitrogen atom weakens C=N double bonds. Extensive studies² have shown that the *s* character of the nitrogen lone pair in the –N bond increases upon coordination, producing a shorter C=N bond length and a greater –N stretching force constant (higher frequency of vibration). Three medium to strong peaks observed in the range of 1570–1454 cm⁻¹ are likely to be associated with the pyridine rings. A medium to weak metal-sensitive stretching band at 416–411 cm⁻¹ for all complexes can be assigned to the ν_{M-N} vibration. For hexadentate ligands (**L⁵** and **L⁶**) and corresponding complexes, the ν_{C-O} stretching vibration is observed at 1290 cm⁻¹.

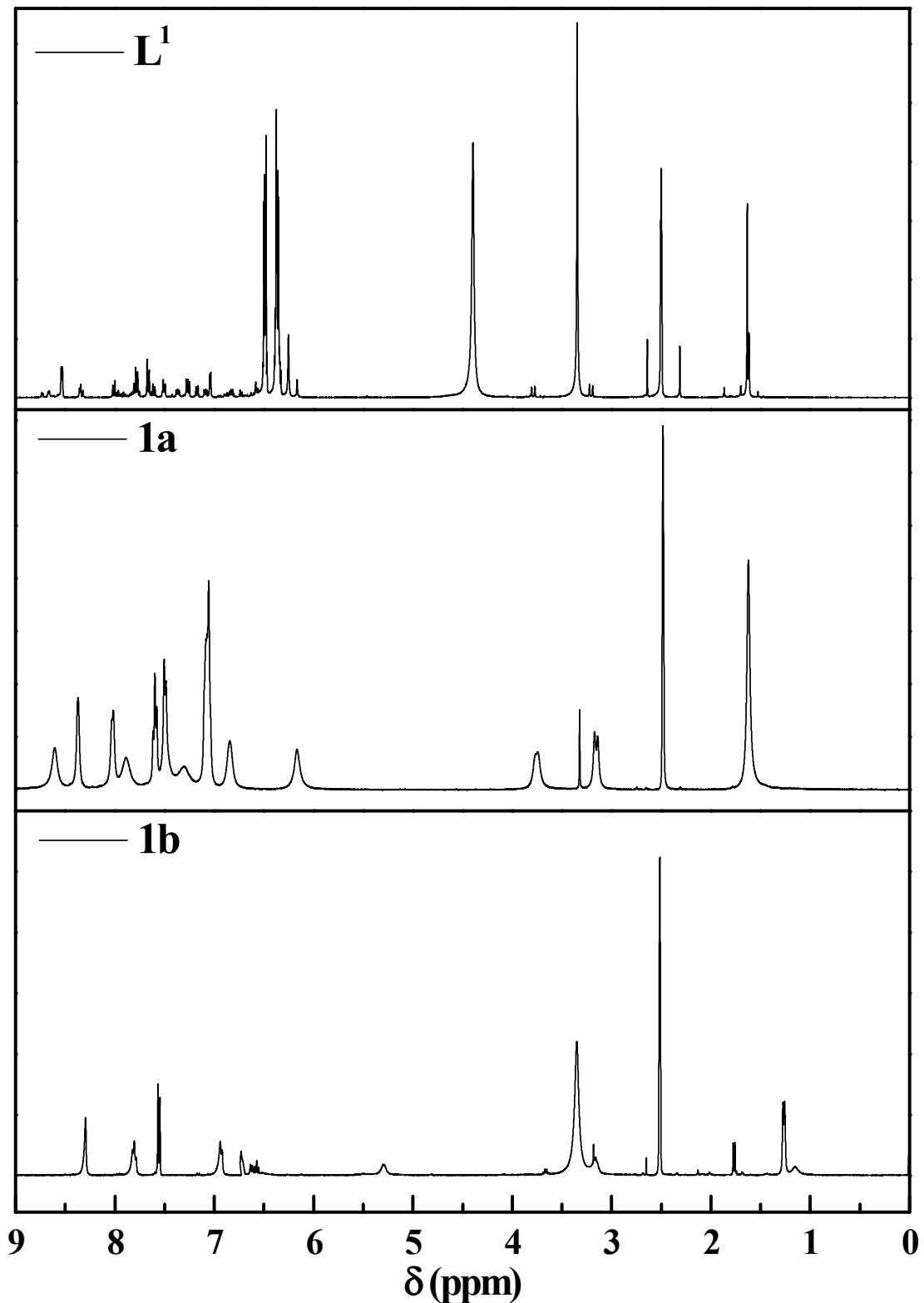


Fig. S4 ^1H NMR spectra of \mathbf{L}^1 , $\mathbf{1a}$ and $\mathbf{1b}$.

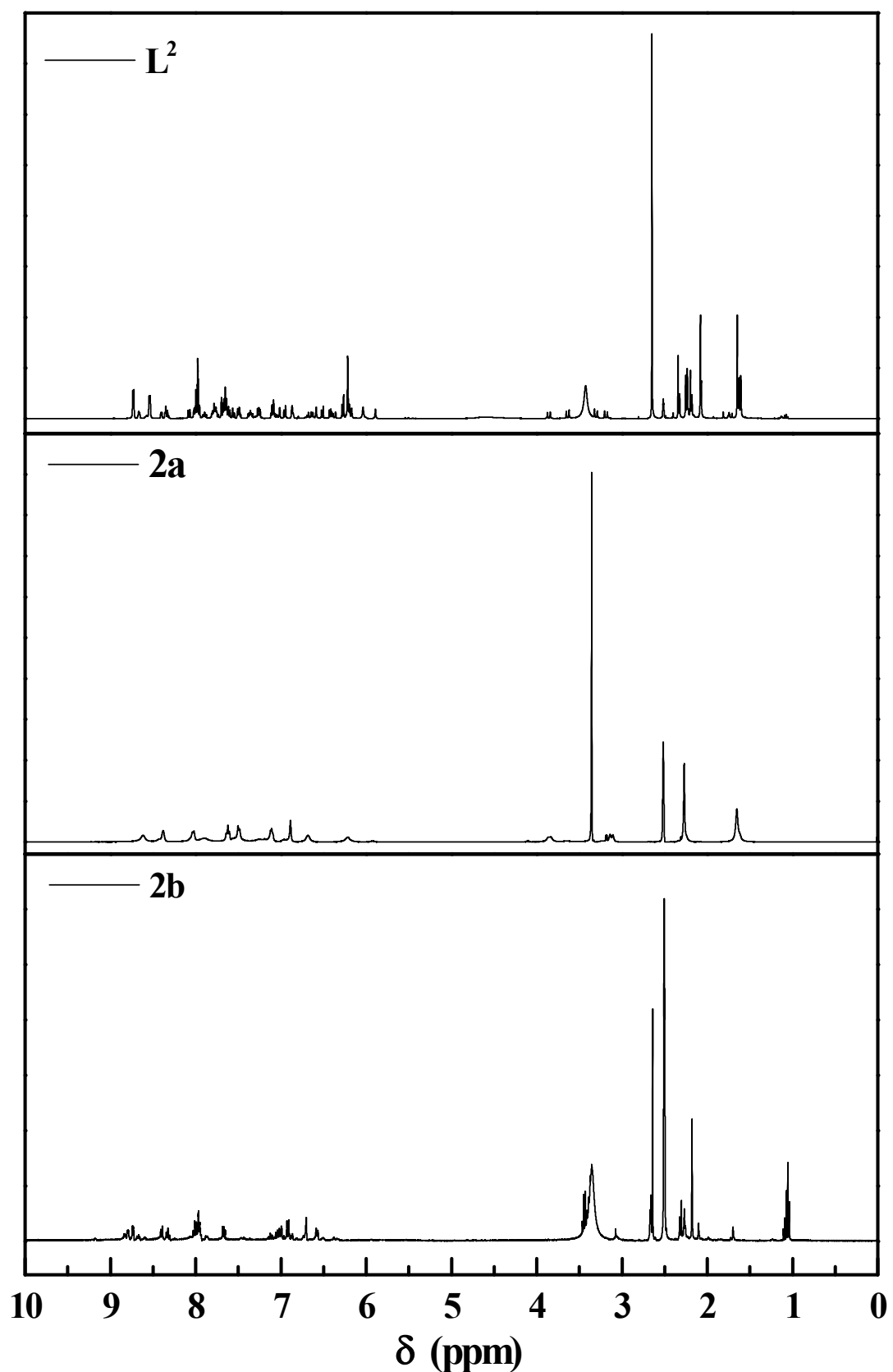


Fig. S5 ^1H NMR spectra of L^2 , **2a** and **2b**.

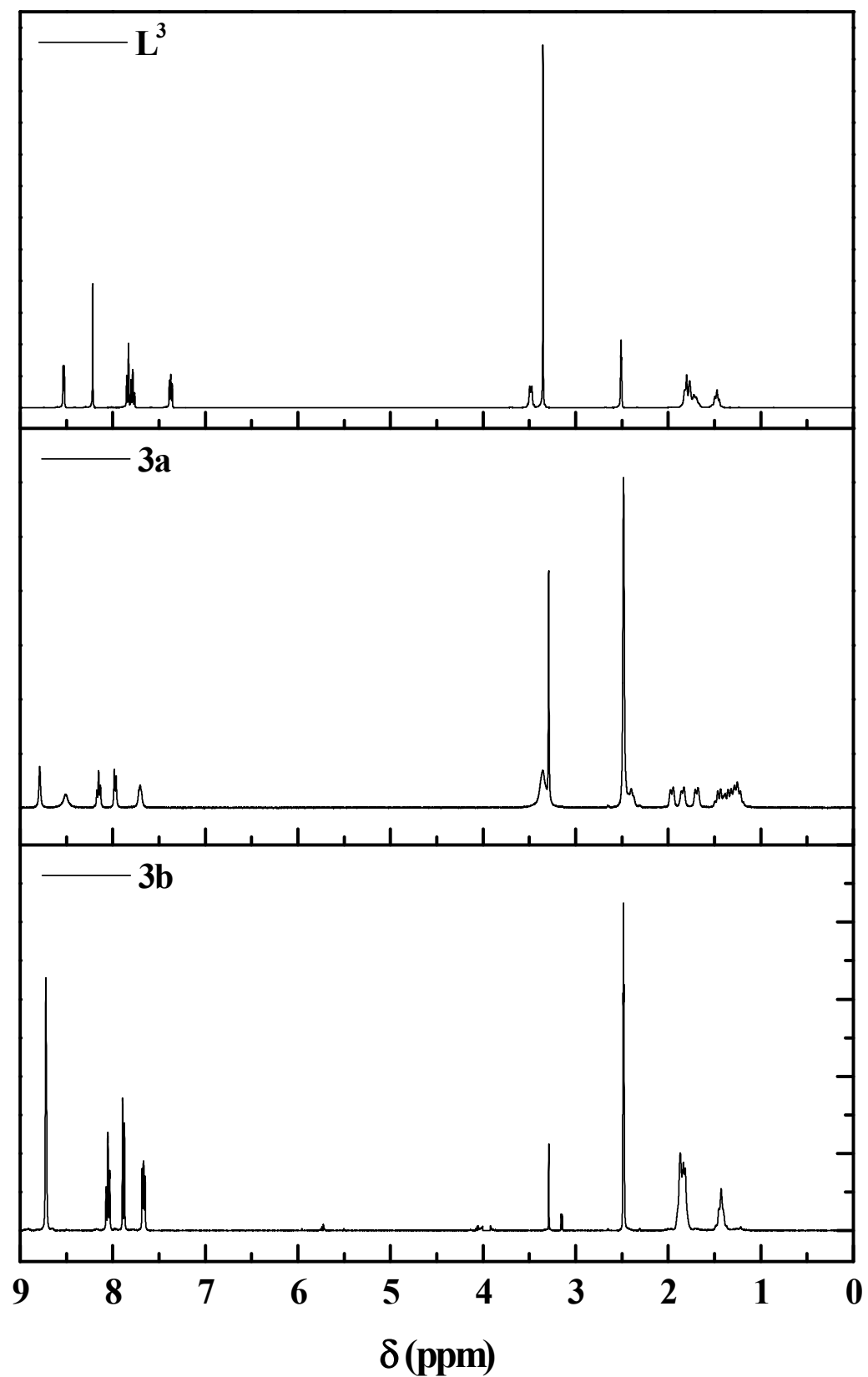


Fig. S6 ^1H NMR spectra of L^3 , 3a and 3b .

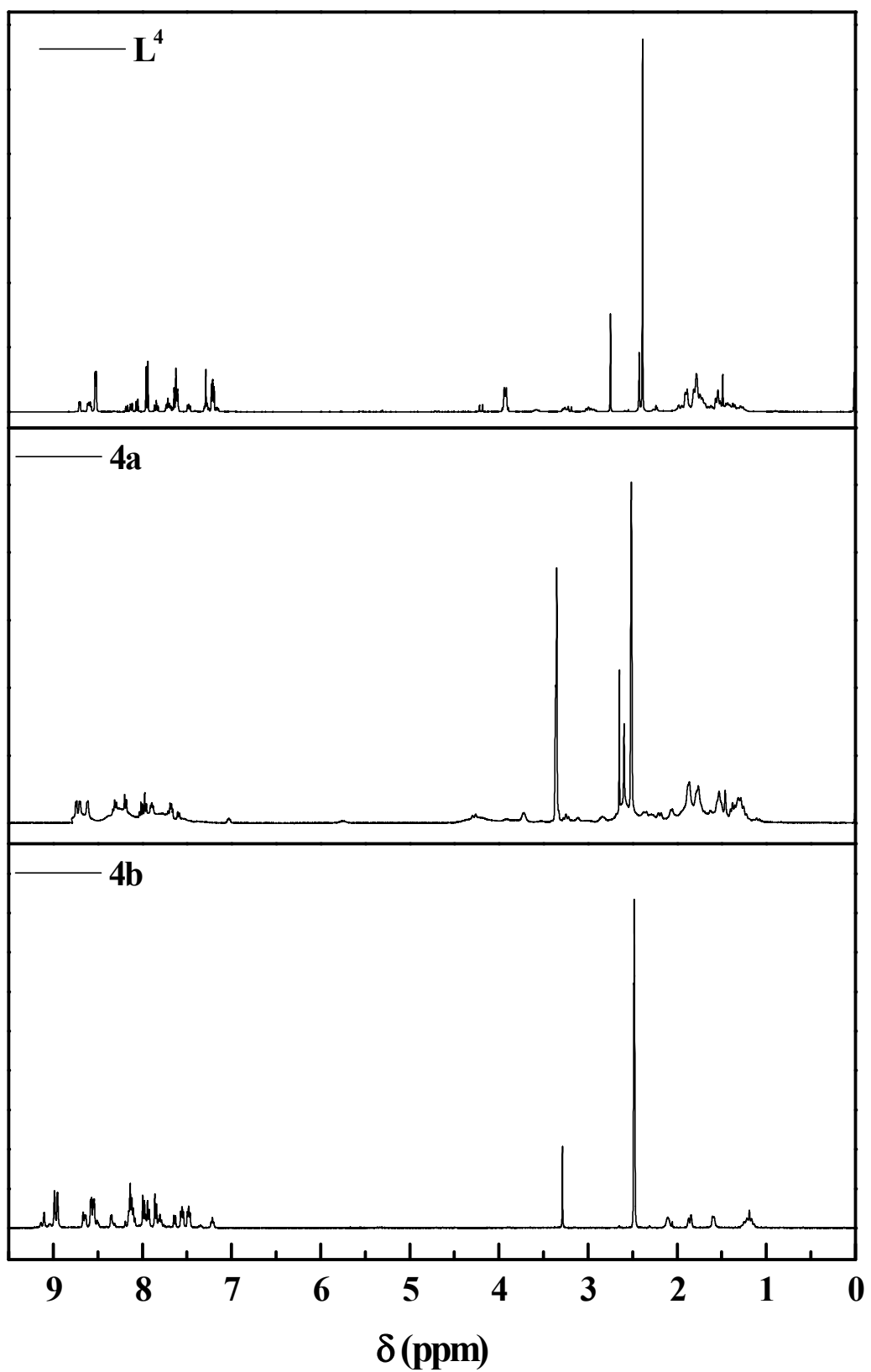


Fig. S7 ^1H NMR spectra of L^4 , 4a and 4b .

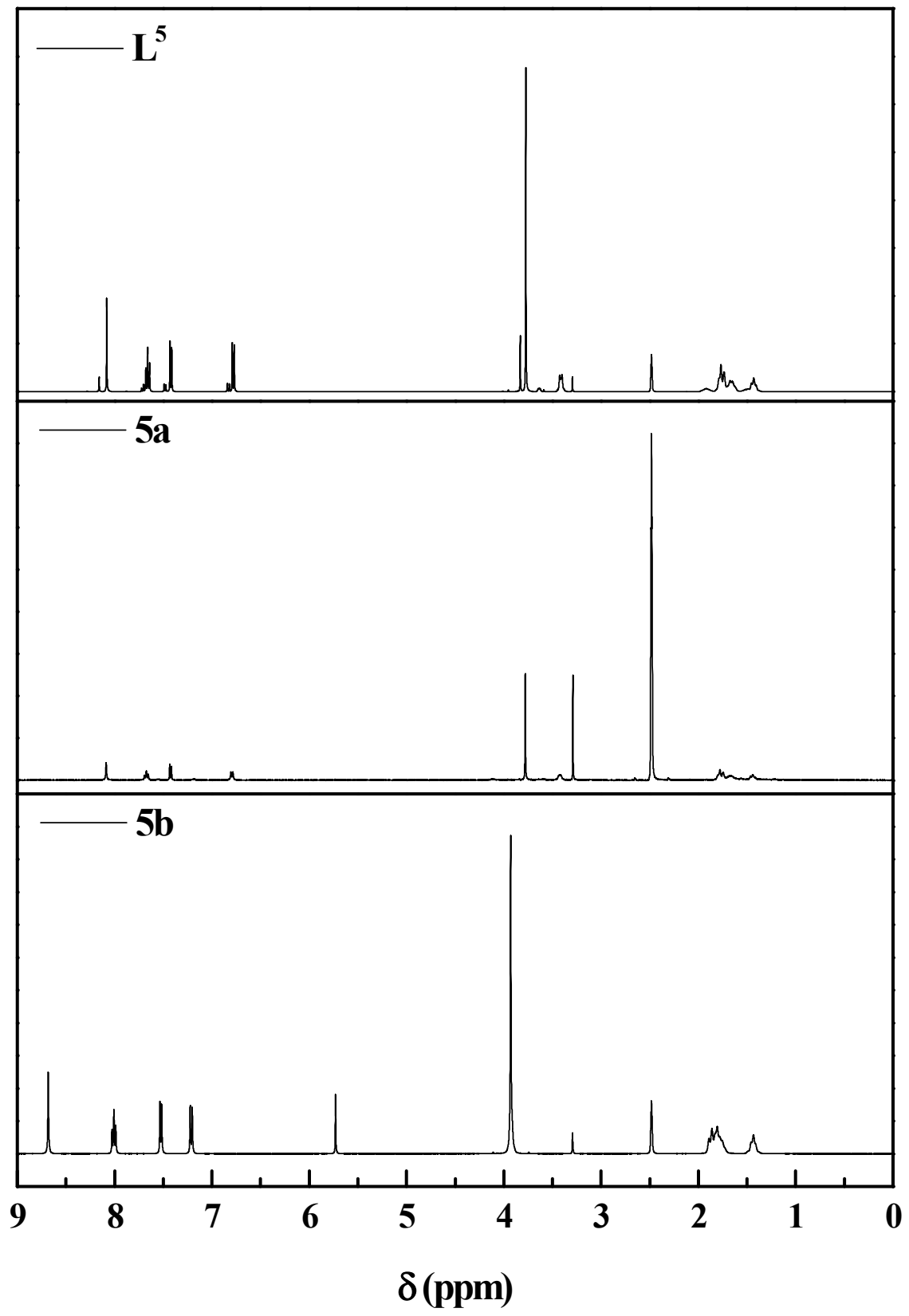


Fig. S8 ^1H NMR spectra of \mathbf{L}^5 , $\mathbf{5a}$ and $\mathbf{5b}$.

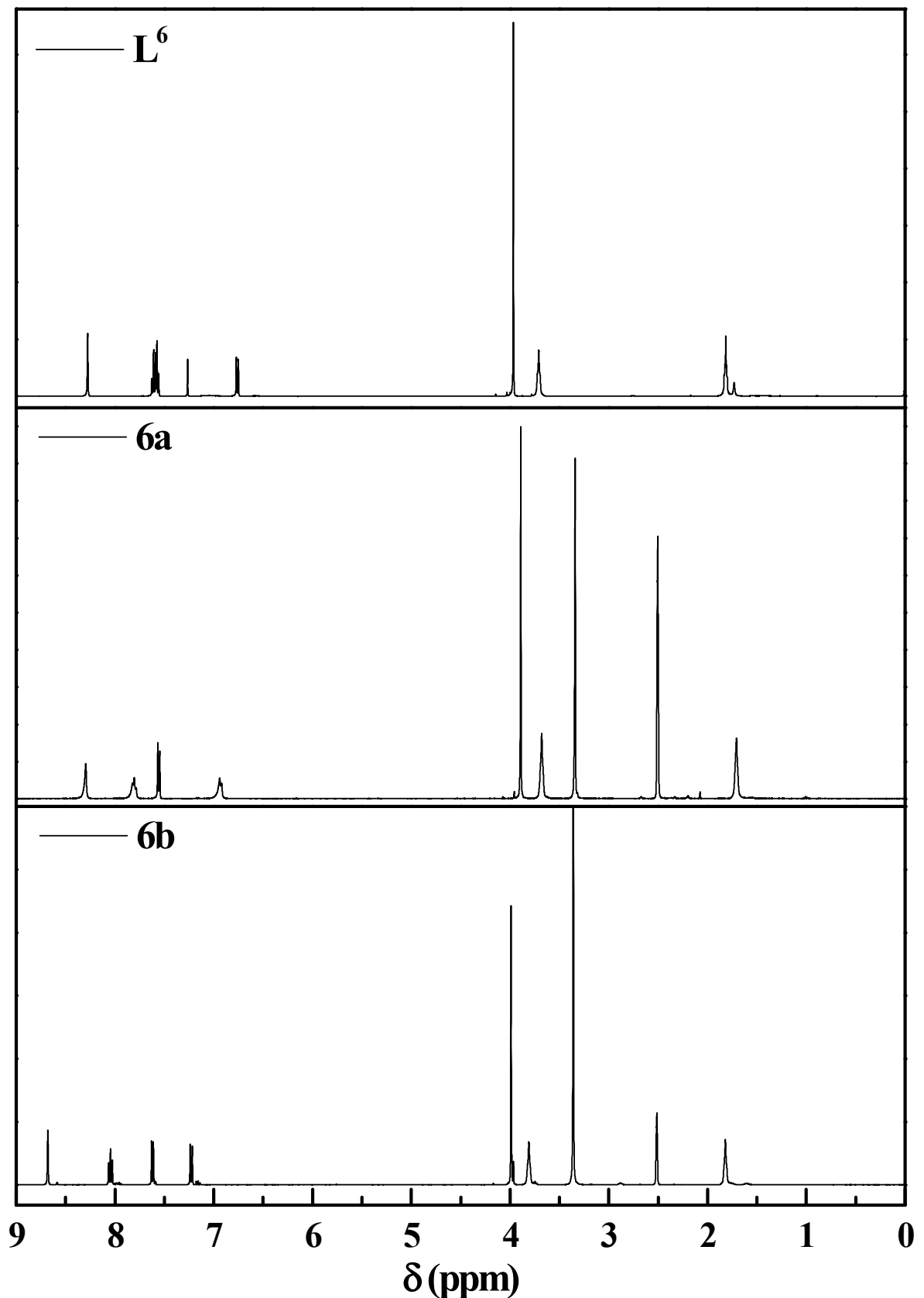


Fig. S9 ^1H NMR spectra of L^6 , **6a** and **6b**.

¹H NMR characteristics.

The ¹H NMR spectra of ligands and complexes have been recorded to probe the solution structure (Figures S4–S9). The six or eight protons on two pyridine rings do not exhibit spin structure and display an upfield shift in the order of *o* (ortho), *m* (meta), *p* (para), which appear as broad signal at *ca.* 6.75–8.54 δ . Further, these signals display a downfield shift due to the coordination by the imine–N and pyridine–N. This behavior causes a characteristic change of chemical shift of the proton resonances compared to that in the free ligands. Only one set of protons corresponding to the imine –CH=N– moieties of the ligands (**L**², **L**⁵ and **L**⁶) and complexes appear in the range 8.12–8.84 δ . For **L**³, **L**⁴, **L**⁵ and corresponding complexes, appearance of cyclohexanediyl protons of –CH₂– group and –CH– group as solitary signal unambiguously testifies that the ligands and complexes are magnetically equivalent. The multiplet at the lower field is assigned to the –CH– group protons attached to the imine nitrogen and the multiplet at higher field is assigned to the –CH₂– group protons. Their chemical shift was observed at *ca.* 1.8 ppm. For the corresponding complexes of **L**¹, **L**², and **L**⁴, the methyl resonance is observed at 3.5 ppm as a sharp singlet as expected. Especially for **L**² and corresponding complexes, the resonance of substituent methyl on benzene resonance is performed at 2.31 ppm. For hexadentate ligands (**L**⁵ and **L**⁶) and corresponding complexes, the obvious signal at *ca.* 3.8 ppm is assigned to the –OCH₃ group protons. For **L**⁶ and corresponding complexes, sharp singlets at δ = 3.6 and 1.7 ppm due to eight methylene protons, which is fully consistent with the crystallographically imposed mirror symmetry.

Table S1 Selected bond lengths [Å] and angles [°] for **[Zn(L¹)Cl₂] (1a)**.

Zn(1)-N(3)	2.066(5)	Zn(1)-Cl(1)	2.1990(17)	C(1)-N(3)	1.332(7)
Zn(1)-N(2)	2.067(4)	Zn(1)-Cl(2)	2.2066(17)	C(5)-N(3)	1.349(7)
C(6)-N(2)	1.296(7)	C(8)-N(2)	1.417(6)	C(13)-N(1)	1.402(7)
C(14)-N(1)	1.452(8)	C(16)-N(4)	1.316(7)	C(20)-N(4)	1.332(8)
N(3)-Zn(1)-N(2)	79.68(17)	N(2)-Zn(1)-Cl(1)	114.04(13)	N(2)-Zn(1)-Cl(2)	110.81(13)
N(3)-Zn(1)-Cl(1)	111.19(14)	N(3)-Zn(1)-Cl(2)	115.53(14)	Cl(1)-Zn(1)-Cl(2)	119.15(7)
C(6)-N(2)-Zn(1)	114.7(3)	C(8)-N(2)-Zn(1)	123.0(3)	C(1)-N(3)-Zn(1)	126.4(4)

Table S2 Selected bond lengths [Å] and angles [°] for **[Hg(L¹)Cl₂] (1b)**.

Hg(1)-N(2)	2.294(16)	Hg(1)-Cl(1)	2.405(6)	C(1)-N(4)	1.26(4)
Hg(1)-Cl(2)	2.405(8)	Hg(1)-N(1)	2.442(17)	C(5)-N(4)	1.36(3)
C(7)-N(3)	1.40(3)	C(9)-N(1)	1.25(3)	C(10)-N(2)	1.36(3)
C(14)-N(2)	1.34(3)	C(15)-N(1)	1.43(2)	C(20)-N(3)	1.40(3)
N(2)-Hg(1)-Cl(2)	122.8(5)	N(2)-Hg(1)-Cl(1)	118.9(5)	Cl(2)-Hg(1)-Cl(1)	113.9(3)
N(2)-Hg(1)-N(1)	71.0(6)	Cl(2)-Hg(1)-N(1)	100.1(4)	Cl(1)-Hg(1)-N(1)	120.6(5)
C(9)-N(1)-Hg(1)	112.8(13)	C(15)-N(1)-Hg(1)	125.1(13)	C(14)-N(2)-Hg(1)	121.4(13)
C(10)-N(2)-Hg(1)	117.1(13)				

Table S3 Selected bond lengths [Å] and angles [°] for **[Zn(L²)Cl₂] (2a)**.

Zn(1)-N(1)	2.052(8)	Zn(1)-Cl(1)	2.189(3)	C(1)-N(2)	1.354(12)
Zn(1)-N(2)	2.055(8)	Zn(1)-Cl(2)	2.201(3)	C(5)-N(2)	1.356(12)
N(1)-Zn(1)-N(2)	79.8(3)	N(1)-Zn(1)-Cl(1)	105.9(2)	N(2)-Zn(1)-Cl(1)	115.9(2)
N(1)-Zn(1)-Cl(2)	120.0(3)	N(2)-Zn(1)-Cl(2)	112.5(2)	Cl(1)-Zn(1)-Cl(2)	117.36(14)
C(6)-N(1)-Zn(1)	114.5(6)	C(7)-N(1)-Zn(1)	123.0(7)	C(1)-N(2)-Zn(1)	127.9(7)

Table S4 Selected bond lengths [Å] and angles [°] for **[Zn₂(L³)Cl₄] (3a)**.

Zn(1)-N(2)	2.042(8)	Zn(1)-Cl(2)	2.162(5)	Zn(2)-N(3)	2.015(9)
Zn(1)-N(1)	2.066(9)	Zn(1)-Cl(1)	2.204(5)	Zn(2)-N(4)	2.048(9)
Zn(2)-Cl(3)	2.177(5)	Zn(2)-Cl(4)	2.198(5)		
N(2)-Zn(1)-N(1)	80.0(4)	N(2)-Zn(1)-Cl(2)	111.8(3)	N(1)-Zn(1)-Cl(2)	117.0(4)
N(2)-Zn(1)-Cl(1)	116.4(3)	N(1)-Zn(1)-Cl(1)	110.3(4)	Cl(2)-Zn(1)-Cl(1)	116.4(2)
N(3)-Zn(2)-N(4)	80.0(4)	N(3)-Zn(2)-Cl(3)	112.1(3)	N(4)-Zn(2)-Cl(3)	116.3(3)
N(3)-Zn(2)-Cl(4)	116.3(3)	N(4)-Zn(2)-Cl(4)	110.3(4)	Cl(3)-Zn(2)-Cl(4)	116.6(2)
C(5)-N(1)-Zn(1)	112.7(8)	C(1)-N(1)-Zn(1)	126.6(10)	C(6)-N(2)-Zn(1)	112.3(8)

C(7)-N(2)-Zn(1)	128.9(7)	C(13)-N(3)-Zn(2)	115.4(8)	C(12)-N(3)-Zn(2)	131.2(7)
C(18)-N(4)-Zn(2)	131.0(9)	C(14)-N(4)-Zn(2)	112.5(8)	O(6)#3-In(2)-O(6)#485.46(11)	

Table S5 Selected bond lengths [Å] and angles [°] for **[Hg₂(L³)Cl₄]·CH₂Cl₂ (3b)**.

Hg(1)-N(1)	2.283(5)	Hg(1)-N(2)	2.482(5)	Hg(1)-Cl(2)	2.5333(16)
Hg(1)-Cl(1)	2.3749(17)	N(1)-C(1)	1.327(8)	N(1)-C(5)	1.352(8)
N(2)-C(6)	1.270(8)	N(2)-C(7)	1.456(8)	C(10)-Cl(3)#1	1.613(13)
N(1)-Hg(1)-Cl(1)	149.50(14)	N(1)-Hg(1)-N(2)	71.27(17)	Cl(1)-Hg(1)-N(2)	107.18(12)
N(1)-Hg(1)-Cl(2)	99.12(13)	Cl(1)-Hg(1)-Cl(2)	110.34(7)	N(2)-Hg(1)-Cl(2)	104.87(12)
C(1)-N(1)-Hg(1)	123.9(4)	C(5)-N(1)-Hg(1)	117.2(4)	C(6)-N(2)-Hg(1)	111.5(4)
C(7)-N(2)-Hg(1)	129.8(4)				

Table S6 Selected bond lengths [Å] and angles [°] for **[Zn₂(L⁴)Cl₄]·CH₃OH (4a)**.

Zn(1)-N(1)	2.050(3)	Zn(1)-Cl(1)	2.1985(14)	Zn(2)-N(4)	2.042(3)
Zn(1)-N(2)	2.061(3)	Zn(1)-Cl(2)	2.2319(14)	Zn(2)-N(3)	2.070(3)
Zn(2)-Cl(4)	2.2142(15)	Zn(2)-Cl(3)	2.2144(14)		
N(1)-Zn(1)-N(2)	80.43(12)	N(1)-Zn(1)-Cl(1)	109.19(10)	N(2)-Zn(1)-Cl(1)	120.05(8)
N(1)-Zn(1)-Cl(2)	115.01(10)	N(2)-Zn(1)-Cl(2)	120.65(9)	Cl(1)-Zn(1)-Cl(2)	117.09(6)
N(4)-Zn(2)-N(3)	80.25(11)	N(4)-Zn(2)-Cl(4)	70.58(10)	N(3)-Zn(2)-Cl(4)	110.30(9)
N(4)-Zn(2)-Cl(3)	105.03(10)	N(3)-Zn(2)-Cl(3)	117.33(9)	Cl(4)-Zn(2)-Cl(3)	117.90(6)
C(1)-N(1)-Zn(1)	127.6(3)	C(5)-N(1)-Zn(1)	112.7(2)	C(6)-N(2)-Zn(1)	114.8(2)
C(8)-N(2)-Zn(1)	124.3(2)	C(15)-N(3)-Zn(2)	114.0(2)	C(13)-N(3)-Zn(2)	125.49(19)
C(16)-N(4)-Zn(2)	113.5(2)	C(20)-N(4)-Zn(2)	126.8(3)	O(6)#3-In(2)-O(6)#485.46(11)	

Table S7 Selected bond lengths [Å] and angles [°] for **L⁵**.

C(1)-O(1)	1.414(4)	C(6)-N(1)	1.256(4)	C(8)-N(2)	1.464(4)
C(2)-O(1)	1.355(4)	C(7)-N(2)	1.354(4)	C(2)-N(1)	1.314(4)
N(1)-C(2)-O(1)	119.8(3)	O(1)-C(2)-C(3)	115.7(3)	N(2)-C(7)-C(6)	122.3(3)
N(1)-C(2)-C(3)	124.5(3)	N(1)-C(6)-C(5)	122.4(3)	N(2)-C(8)-C(9)	109.0(3)
C(2)-N(1)-C(6)	117.0(3)	N(1)-C(6)-C(7)	114.5(3)	N(2)-C(8)-C(8)#1	108.9(3)
C(7)-N(2)-C(8)	118.1(3)	C(2)-O(1)-C(1)	117.4(2)		

Table S8 Selected bond lengths [Å] and angles [°] for **[Zn₂(L⁵)Cl₄] (5a)**.

Zn(1)-N(2)	2.0726(19)	Zn(1)-Cl(1)	2.2006(9)	N(1)-C(4)	1.276(3)
Zn(1)-N(1)	2.0855(19)	Zn(1)-Cl(2)	2.2054(10)	N(1)-C(3)	1.469(3)

N(2)-C(9)	1.327(3)	N(2)-C(5)	1.354(3)
N(2)-Zn(1)-N(1)	80.39(7)	N(2)-Zn(1)-Cl(1)	116.88(6)
N(2)-Zn(1)-Cl(2)	111.16(6)	N(1)-Zn(1)-Cl(2)	112.29(6)
C(4)-N(1)-Zn(1)	112.36(15)	C(3)-N(1)-Zn(1)	128.37(14)
C(5)-N(2)-Zn(1)	111.94(15)	C(9)-N(2)-Zn(1)	128.57(16)

Table S9 Selected bond lengths [Å] and angles [°] for **[Hg₂(L⁵)Cl₄] (5b)**.

Hg(1)-N(1)	2.354(8)	Hg(1)-Cl(7)	2.373(4)	Hg(2)-N(3)	2.333(7)
Hg(1)-Cl(3)	2.360(4)	Hg(1)-N(2)	2.433(7)	Hg(2)-Cl(6)	2.355(3)
Hg(2)-Cl(8)	2.383(3)	Hg(2)-N(4)	2.640(8)		
N(1)-Hg(1)-Cl(3)	104.4(2)	N(1)-Hg(1)-Cl(7)	111.9(2)	Cl(3)-Hg(1)-Cl(7)	137.15(13)
N(1)-Hg(1)-N(2)	70.1(3)	Cl(3)-Hg(1)-N(2)	107.5(2)	Cl(7)-Hg(1)-N(2)	105.8(2)
N(3)-Hg(2)-Cl(6)	108.76(19)	N(3)-Hg(2)-Cl(8)	108.3(2)	Cl(6)-Hg(2)-Cl(8)	142.69(11)
N(3)-Hg(2)-N(4)	70.3(2)	Cl(6)-Hg(2)-N(4)	104.11(19)	Cl(8)-Hg(2)-N(4)	92.1(2)
C(2)-N(1)-Hg(1)	123.6(7)	C(6)-N(1)-Hg(1)	116.7(6)	C(7)-N(2)-Hg(1)	114.7(6)
C(8)-N(2)-Hg(1)	124.2(6)	C(14)-N(3)-Hg(2)	117.7(6)	C(13)-N(3)-Hg(2)	123.3(6)
C(19)-N(4)-Hg(2)	135.7(7)	C(15)-N(4)-Hg(2)	106.9(5)		

Table S10 Selected bond lengths [Å] and angles [°] for L⁶.

N(2)-C(8)	1.314(3)	O(1)-C(8)	1.354(3)	N(1)-C(3)	1.258(3)
N(2)-C(4)	1.353(3)	O(1)-C(9)	1.429(3)	N(1)-C(2)	1.458(3)
C(8)-N(2)-C(4)	116.8(2)	N(2)-C(4)-C(3)	114.4(2)	O(1)-C(8)-C(7)	116.3(3)
C(8)-O(1)-C(9)	117.7(2)	N(1)-C(3)-C(4)	123.3(3)	N(1)-C(2)-C(1)	111.6(2)
C(3)-N(1)-C(2)	117.4(2)	N(2)-C(8)-O(1)	119.6(2)		
N(2)-C(4)-C(5)	122.8(3)	N(2)-C(8)-C(7)	124.2(3)		

Table S11 Selected bond lengths [Å] and angles [°] for **[Zn₂(L⁶)Cl₄]·4CH₃CN (6a)**.

Zn(1)-N(2)	2.0720(18)	Zn(1)-Cl(1)	2.1975(10)	O(1)-C(5)	1.337(3)
Zn(1)-N(1)	2.0758(18)	Zn(1)-Cl(2)	2.2075(9)	O(1)-C(7)	1.449(3)
N(1)-C(6)	1.264(3)	N(1)-C(8)	1.468(3)	N(2)-C(5)	1.332(3)
N(2)-C(1)	1.356(3)	N(3)-C(11)	1.118(5)	N(4)-C(13)	1.115(4)
N(2)-Zn(1)-N(1)	80.45(7)	N(2)-Zn(1)-Cl(1)	115.51(6)	N(1)-Zn(1)-Cl(1)	112.76(6)
N(2)-Zn(1)-Cl(2)	109.46(5)	N(1)-Zn(1)-Cl(2)	112.52(6)	Cl(1)-Zn(1)-Cl(2)	119.67(4)
C(6)-N(1)-Zn(1)	112.60(15)	C(8)-N(1)-Zn(1)	128.31(15)	C(5)-N(2)-Zn(1)	128.90(15)

C(1)-N(2)-Zn(1) 111.81(14)

Table S12 Selected bond lengths [\AA] and angles [$^\circ$] for $[\text{Hg}_2(\text{L}^6)\text{Cl}_4]$ (**6b**).

Hg(1)-N(2)	2.246(16)	Hg(1)-Cl(1)	2.408(6)	Hg(2)-N(3)	2.259(14)
Hg(1)-Cl(2)	2.385(6)	Hg(1)-N(1)	2.697(15)	Hg(2)-Cl(3)	2.379(7)
Hg(2)-Cl(4)	2.407(6)				
N(2)-Hg(1)-Cl(2)	118.0(5)	N(2)-Hg(1)-Cl(1)	115.8(5)	Cl(2)-Hg(1)-Cl(1)	126.2(2)
N(2)-Hg(1)-N(1)	68.8(5)	Cl(2)-Hg(1)-N(1)	86.6(4)	Cl(1)-Hg(1)-N(1)	112.1(4)
N(3)-Hg(2)-Cl(3)	118.0(4)	N(3)-Hg(2)-Cl(4)	115.4(4)	Cl(3)-Hg(2)-Cl(4)	126.5(2)
C(1)-N(1)-Hg(1)	134.2(14)	C(5)-N(1)-Hg(1)	103.3(12)	C(6)-N(2)-Hg(1)	121.4(12)
C(7)-N(2)-Hg(1)	121.9(13)	C(11)-N(3)-Hg(2)	118.1(12)	C(10)-N(3)-Hg(2)	119.8(12)

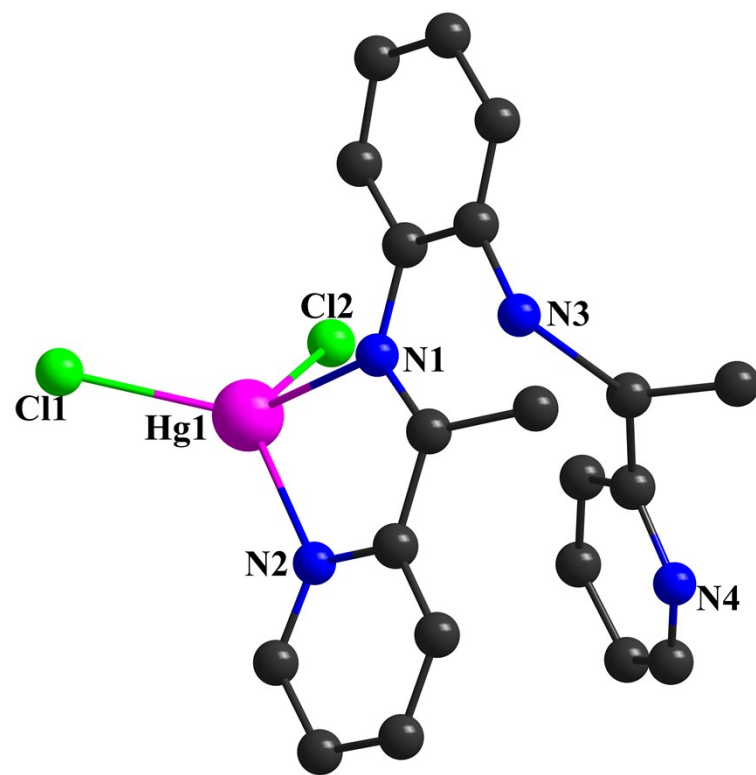


Fig. S10 Perspective view of the asymmetric unit of $[\text{Hg}(\text{L}^1)\text{Cl}_2]$ (**1b**); H atoms are not shown for clarity.

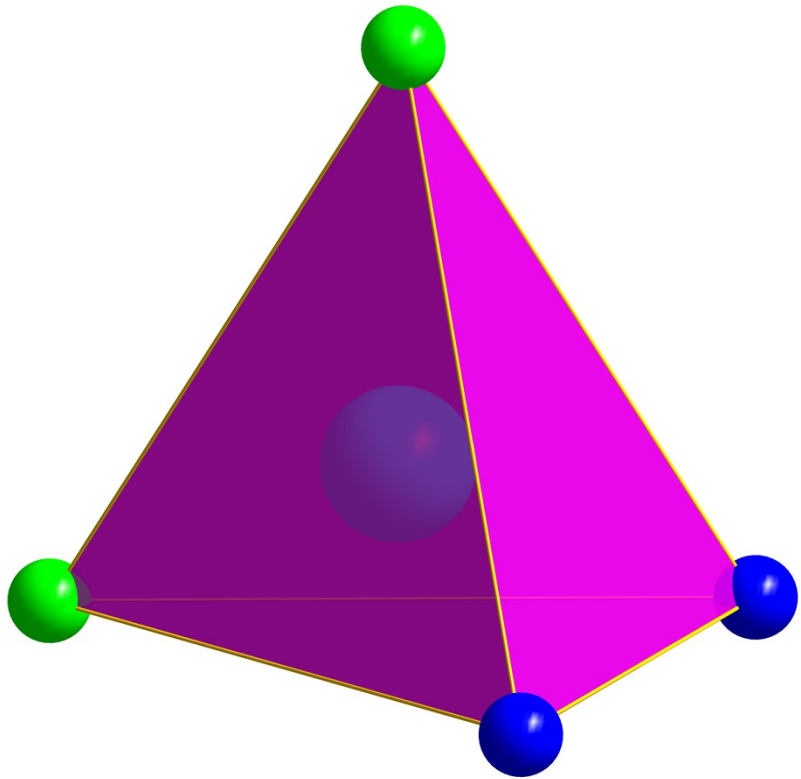


Fig.S11 The coordinating polyhedron of **1a**.

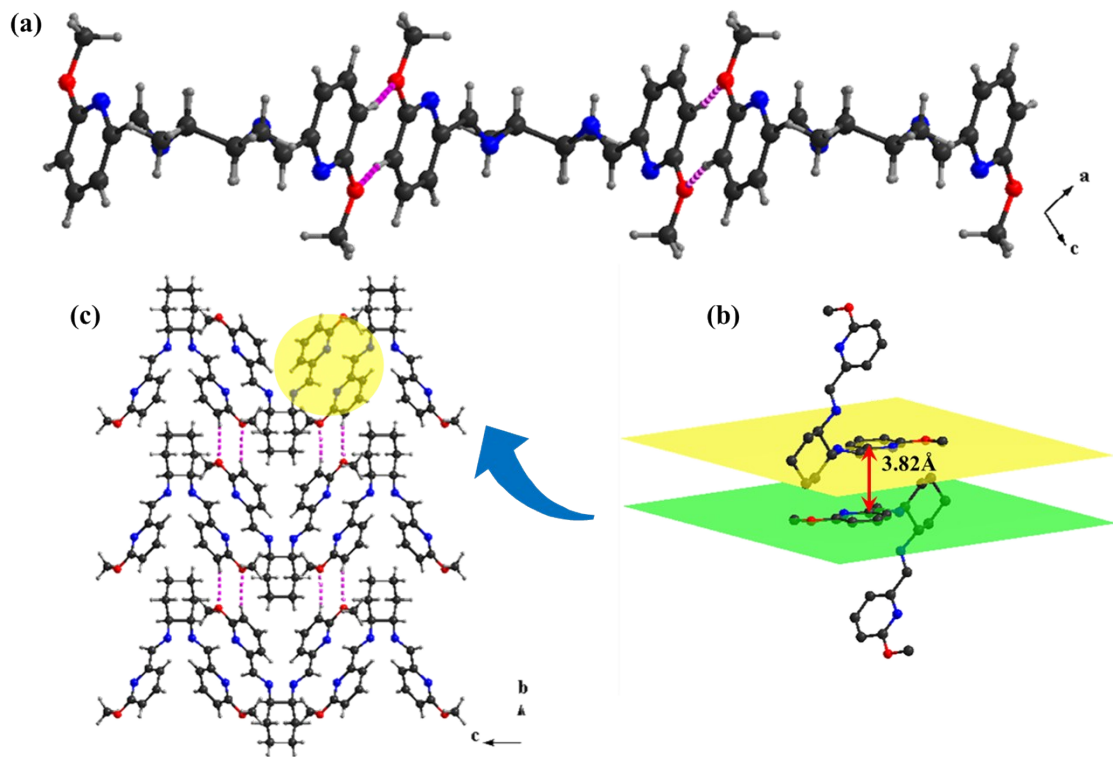


Fig. S12 (a) The infinite chain of \mathbf{L}^5 generated through $\text{C}-\text{H}\cdots\text{O}$ hydrogen bonding contacts. (b) The π -stacking interaction in \mathbf{L}^5 . (c) The 2D supramolecular structure of \mathbf{L}^5 .

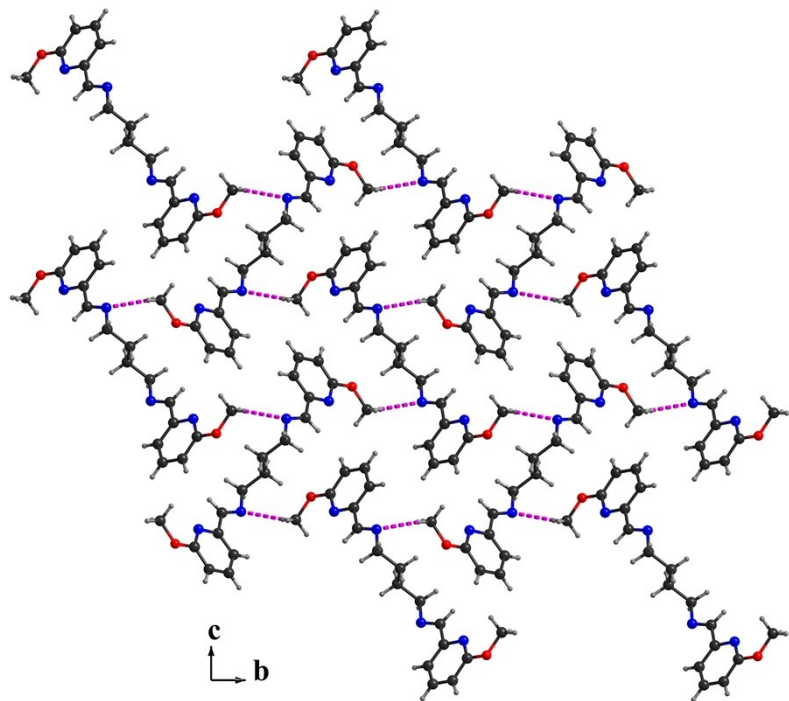


Fig. S13 (a) The 2D supramolecular structure of \mathbf{L}^6 generated through $\text{C}-\text{H}\cdots\text{N}$ hydrogen bonding contacts.

Table S13 Photoluminescent Data for **L¹–L⁶, 1a–6a and 1b–6b** at 298 K

Compound	Absorption (ε) ^a (nm, dm ³ mol ⁻¹ cm ⁻¹)	Emission (λ_{max} , nm)	CIE 1931 (x, y)	(τ , μs) ^b	Φ ^{a,c}	Conditions ^a
L¹	235 (79842); 325 (22285)	571	0.43, 0.41	8.13	0.05	CH ₂ Cl ₂
		582	0.36, 0.49	6.85		Solid state
L²	237 (97585); 326(22285)	544	0.53, 0.47	7.62	0.06	CH ₂ Cl ₂
		547	0.35, 0.47	9.53		Solid state
L³	234 (42437); 266 (23012)	441 ^{sh} ,487	0.22, 0.44	8.32	0.04	CH ₂ Cl ₂
		492	0.29, 0.44	6.13		Solid state
L⁴	235 (45730); 269 (33369)	461 ^{sh} ,487	0.21, 0.52	8.87	0.04	CH ₂ Cl ₂
		496	0.22, 0.32	7.56		Solid state
L⁵	230 (41887); 297 (54169)	472	0.21, 0.52	9.31	0.07	CH ₂ Cl ₂
		513	0.25, 0.32	8.79		Solid state
L⁶	242 (57117); 296 (88279)	402	0.17, 0.11	13.42	0.05	CH ₂ Cl ₂
		419	0.20, 0.27	7.87		Solid state

1a	240 (57748); 331 (22796)	618	0.55, 0.45	7.27	0.25	CH ₂ Cl ₂
		623	0.61, 0.39	9.31		Solid state
2a	242 (79234) 342 (33071)	639	0.55, 0.44	6.78	0.25	CH ₂ Cl ₂
		647	0.59, 0.40	7.81		Solid state
3a	235 (58591); 287 (81962)	548	0.19, 0.47	6.65	0.14	CH ₂ Cl ₂
		528	0.23, 0.30	7.92		Solid state
4a	240 (58265); 284 (47544)	500	0.29, 0.61	5.97	0.15	CH ₂ Cl ₂
		535	0.27, 0.40	7.68		Solid state
5a	234 (52073); 312 (72504)	527	0.16, 0.62	6.80	0.22	CH ₂ Cl ₂
		548	0.27, 0.55	6.42		Solid state
6a	243 (80138); 310 (45957)	429	0.16, 0.04	6.02	0.23	CH ₂ Cl ₂
		442	0.16, 0.07	5.98		Solid state
1b	251 (60907); 333 (25955)	600	0.52, 0.46	7.25	0.19	CH ₂ Cl ₂
		618	0.67, 0.33	4.25		Solid state

2b	253 (56510); 338 (44837)	627	0.46, 0.46	8.08	0.19	CH ₂ Cl ₂
		633	0.63, 0.34	6.22		Solid state
3b	237 (92645); 282 (30199)	536	0.22, 0.56	5.55	0.04	CH ₂ Cl ₂
		545	0.28, 0.43	10.20		Solid state
4b	236 (64186); 284 (17939)	516	0.23, 0.53	8.72	0.05	CH ₂ Cl ₂
		554	0.29, 0.43	6.01		Solid state
5b	239 (83857); 310 (43360)	531	0.18, 0.65	6.96	0.15	CH ₂ Cl ₂
		537	0.31, 0.56	10.32		Solid state
6b	242 (56291); 309 (26687)	434	0.17, 0.05	7.87	0.16	CH ₂ Cl ₂
		442	0.18, 0.15	8.01		Solid state

^aRecorded in dichloromethane at 298 K, concentration = 10⁻⁶ mol L⁻¹; ^bDecay mean lifetime; ^cQuantum yields.

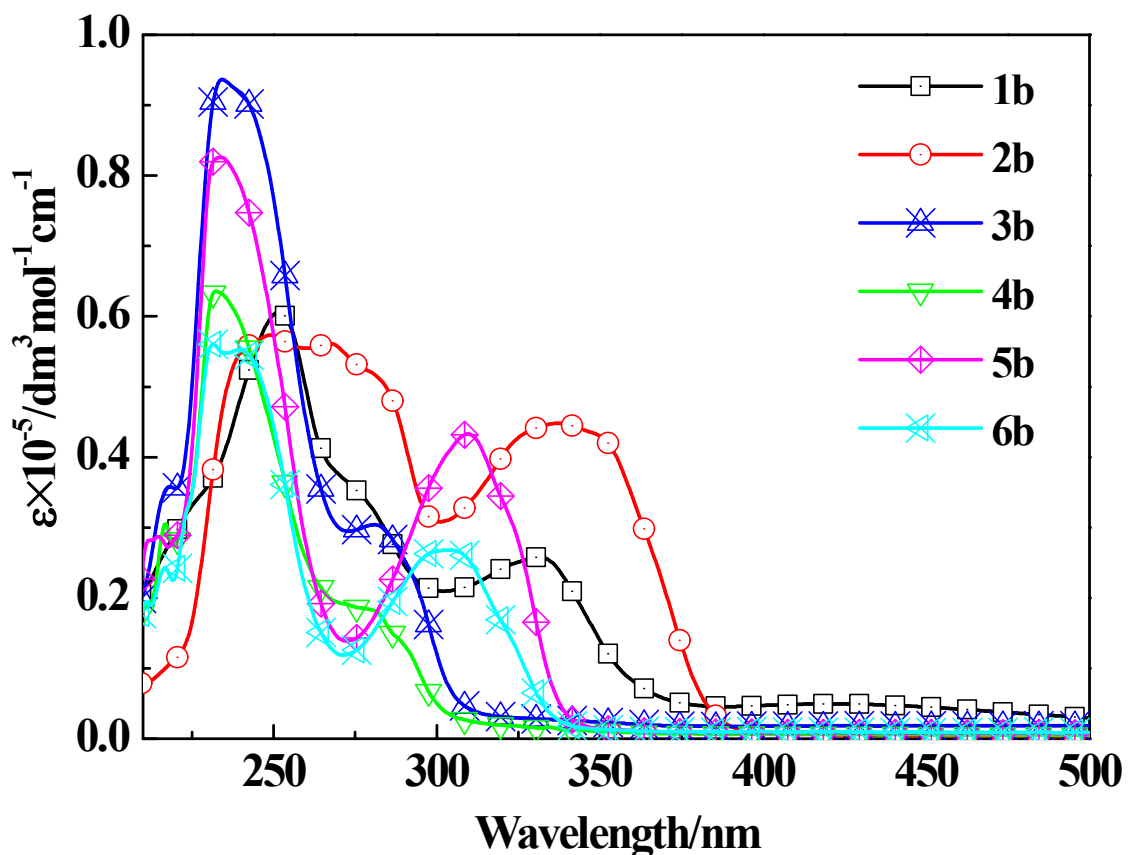


Fig. S14 UV-Vis absorption spectra of complexes **1b**–**6b**

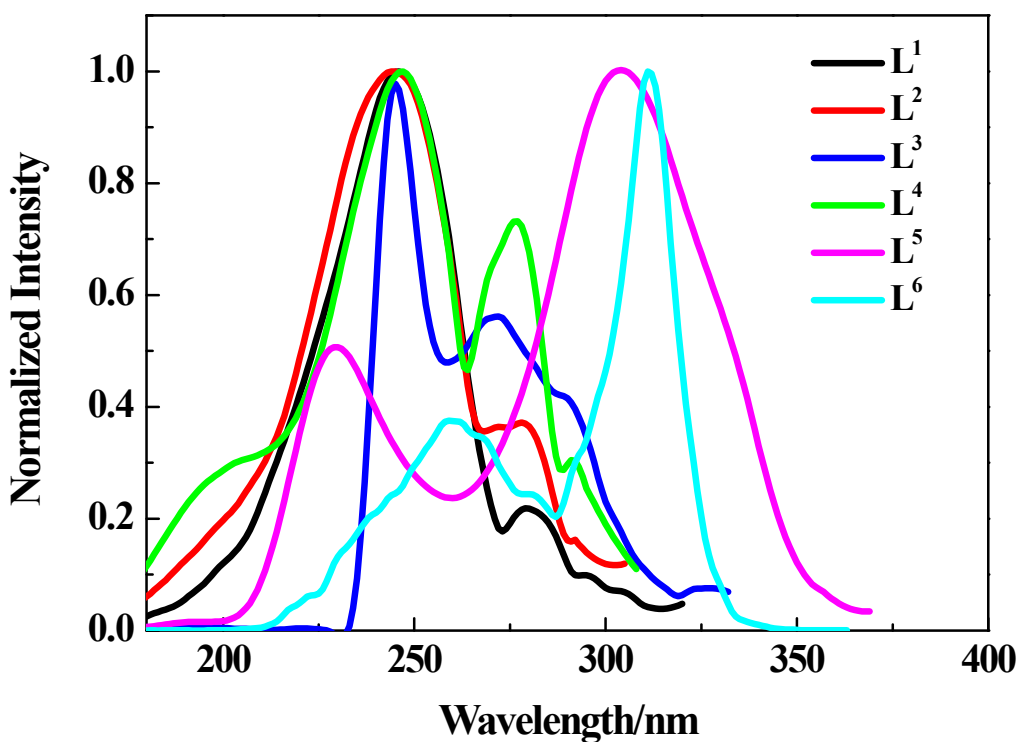


Fig. S15 CH₂Cl₂ solution excitation spectra of free ligands **L**¹–**L**⁶ at 298 K.

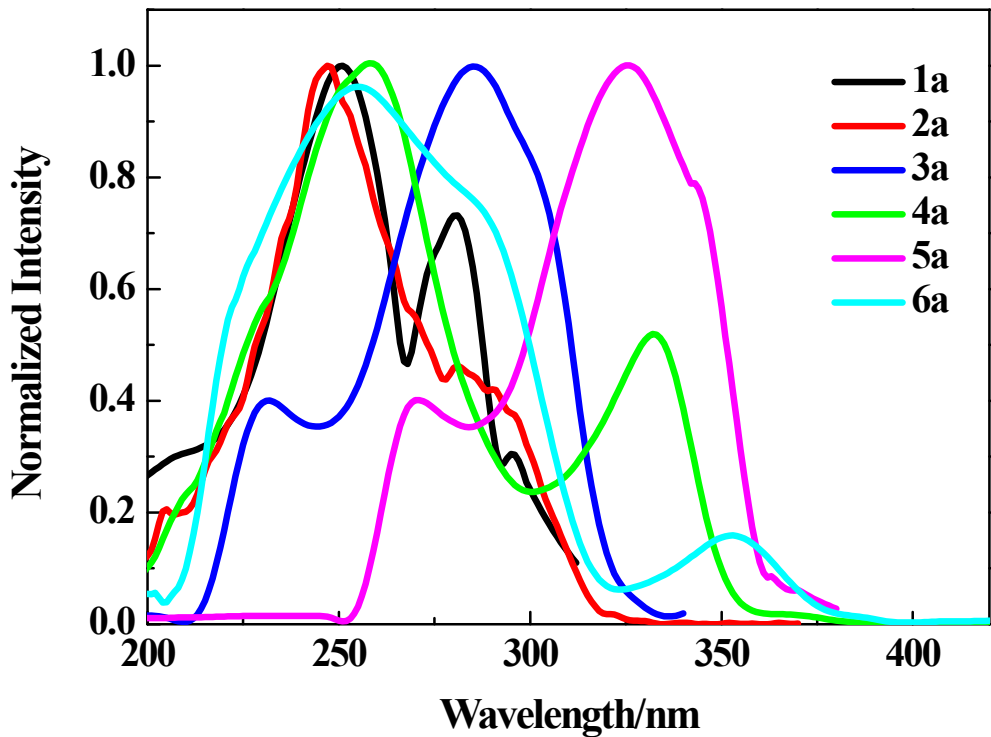


Fig. S16 CH_2Cl_2 solution excitation spectra of **1a–6a** at 298 K.

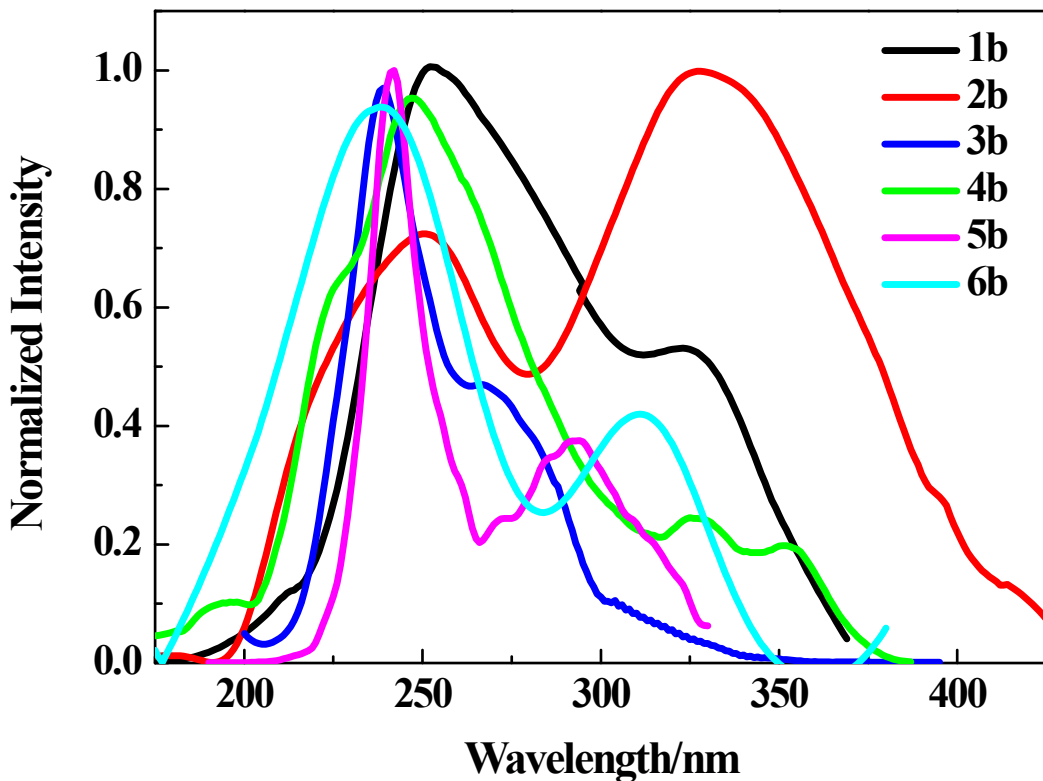


Fig. S17 CH_2Cl_2 solution excitation spectra of **1b–6b** at 298 K.

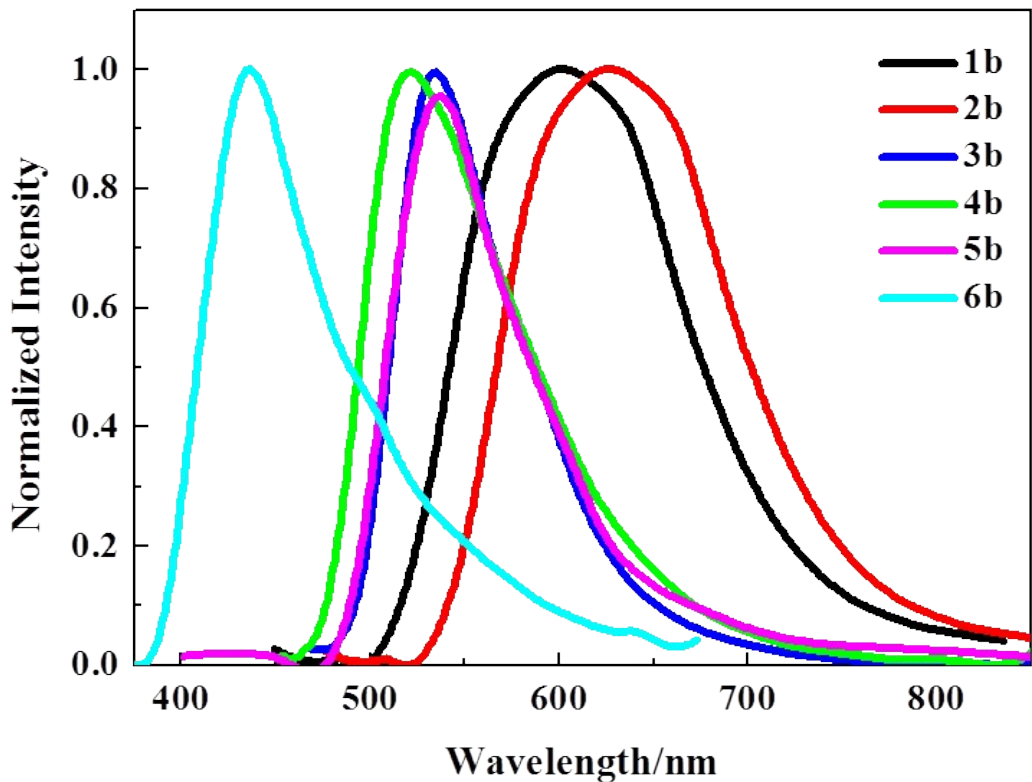


Fig. S18 Emission spectrum of complexes **1b–6b** (1.0×10^{-6} M) at 298 K in CH_2Cl_2 solution.

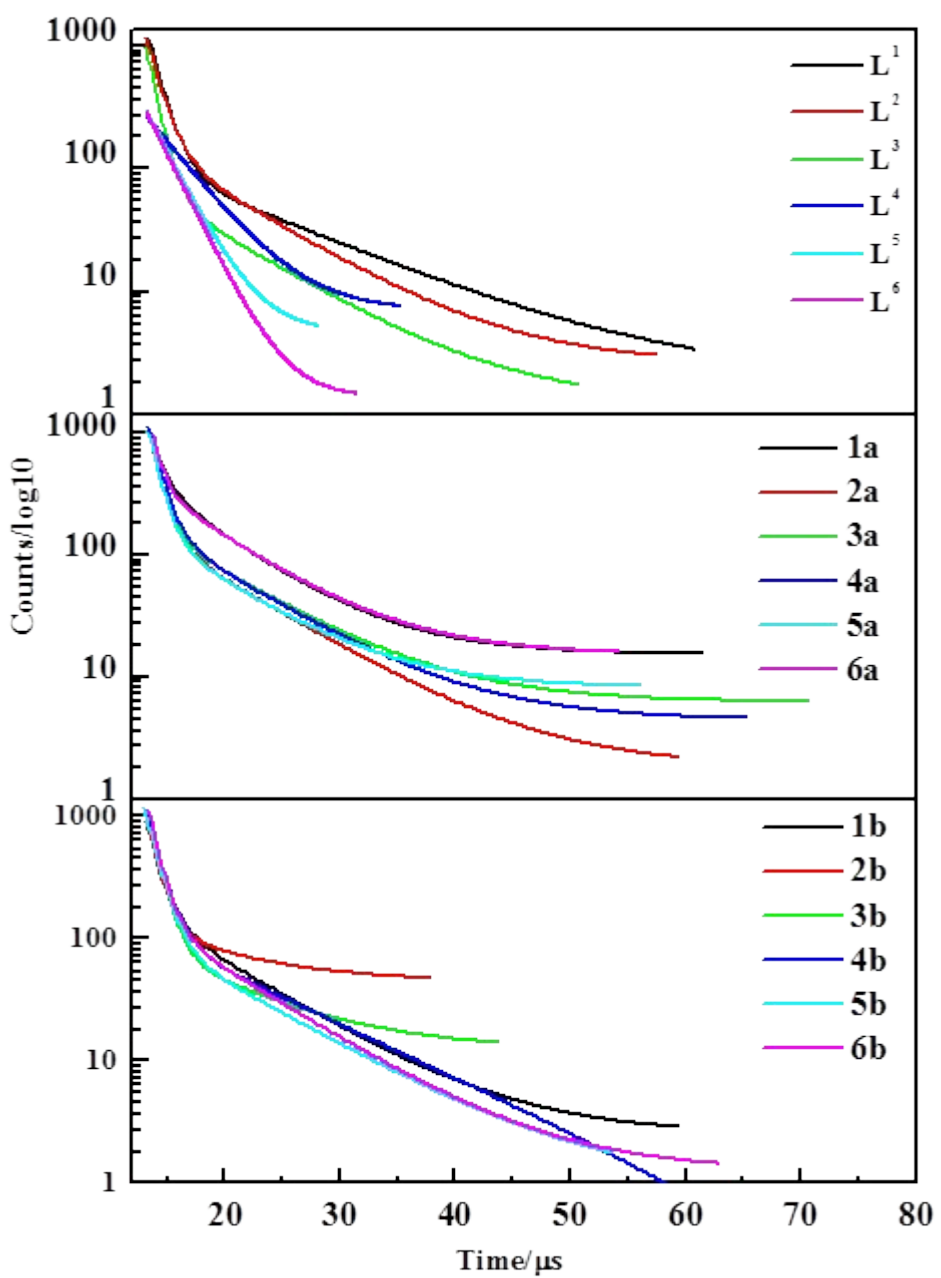


Fig. S19 The luminescence decay curves of Schiff base ligands L^1 - L^6 and complexes $1a$ - $6a$ and $1b$ - $6b$ in CH_2Cl_2 at 298 K.

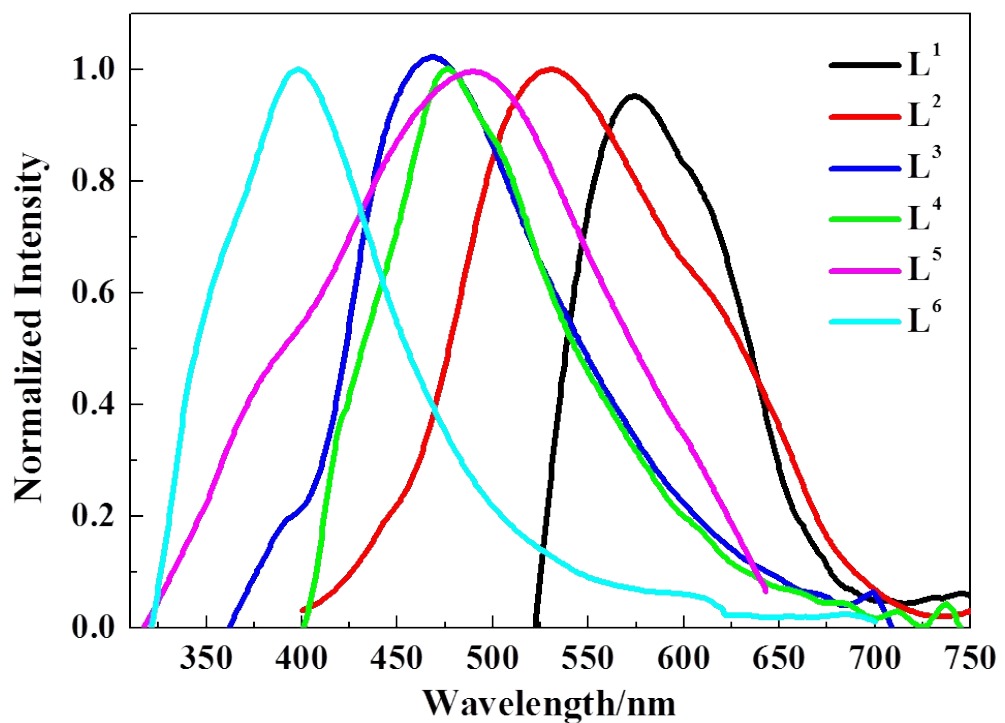


Fig. S20 Solid state emission spectra of free ligands L^1 - L^6 at 298 K

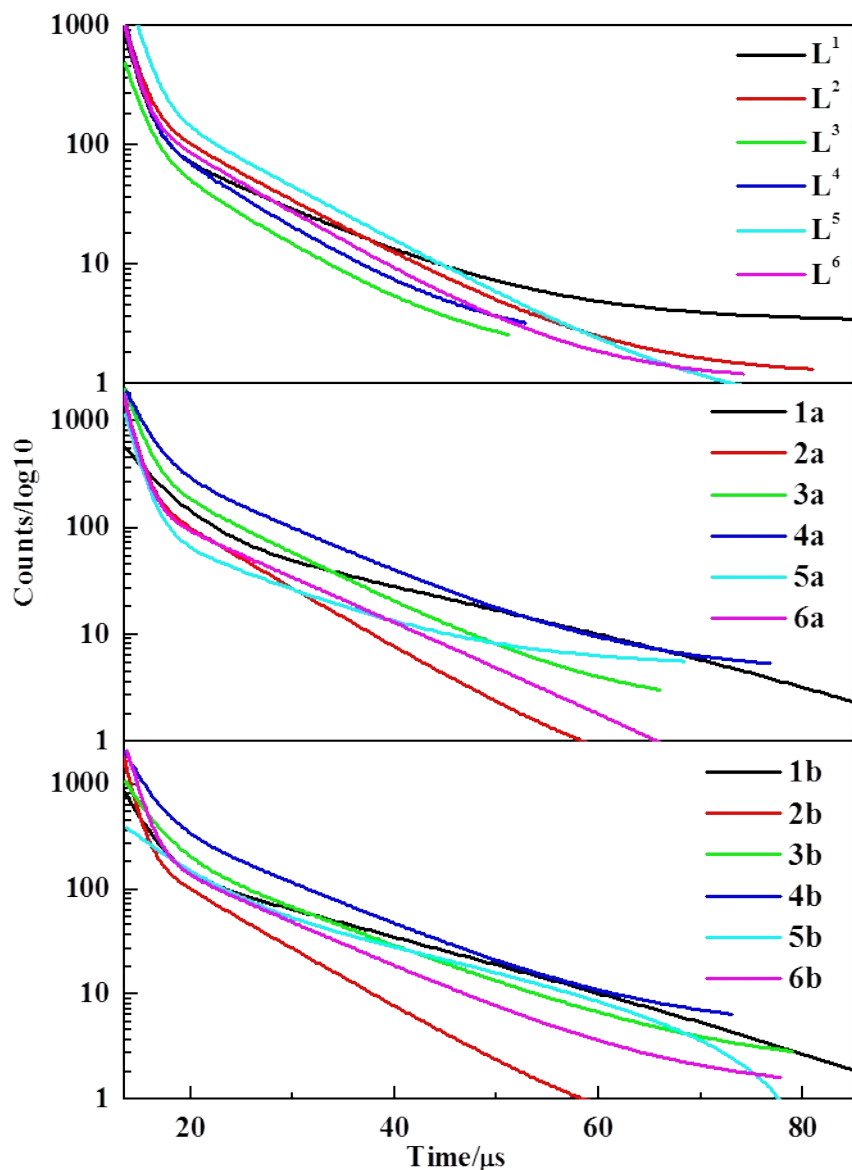


Fig. S21 The luminescence decay curves of Schiff base ligands L^1 - L^6 and complexes **1a-6a** and **1b-6b** in solid state at 298 K

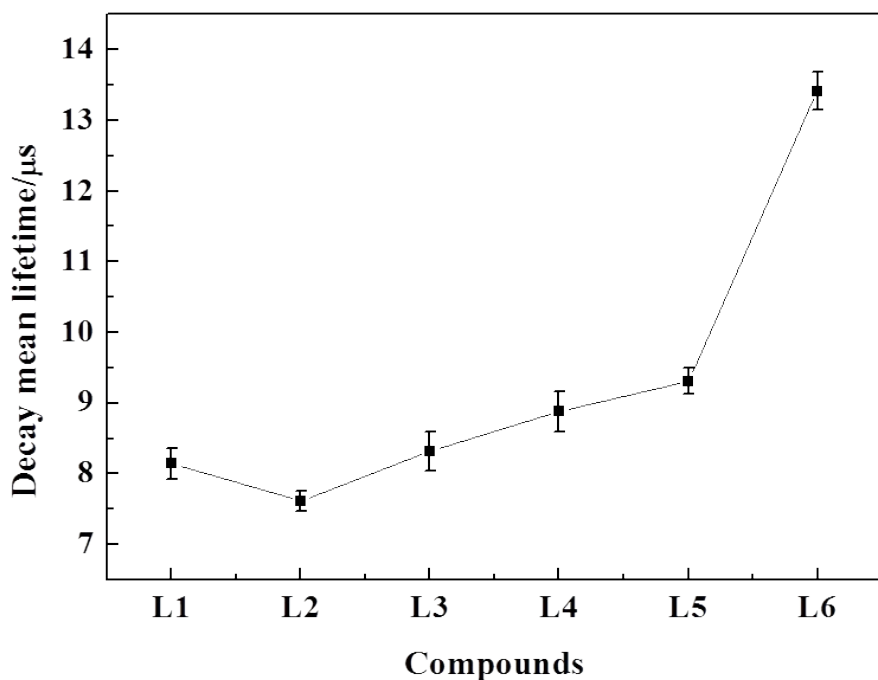


Fig. S22 Error bars for the values of $\mathbf{L}^1\text{--}\mathbf{L}^6$ emission lifetimes in CH_2Cl_2 at 298 K.

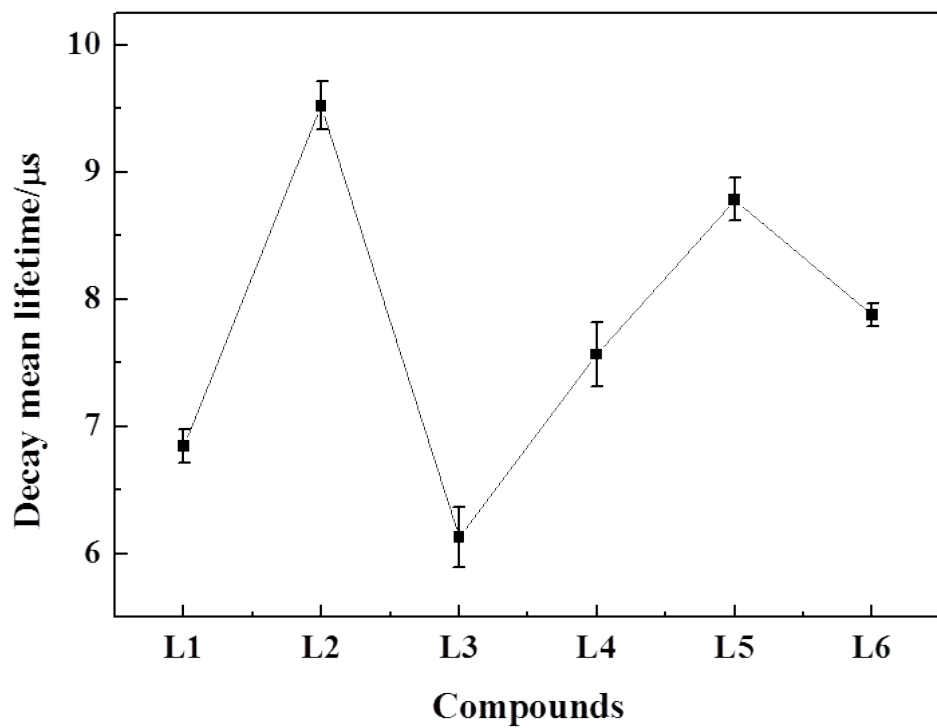


Fig. S23 Error bars for the values of $\mathbf{L}^1\text{--}\mathbf{L}^6$ emission lifetimes in the solid state at 298 K.

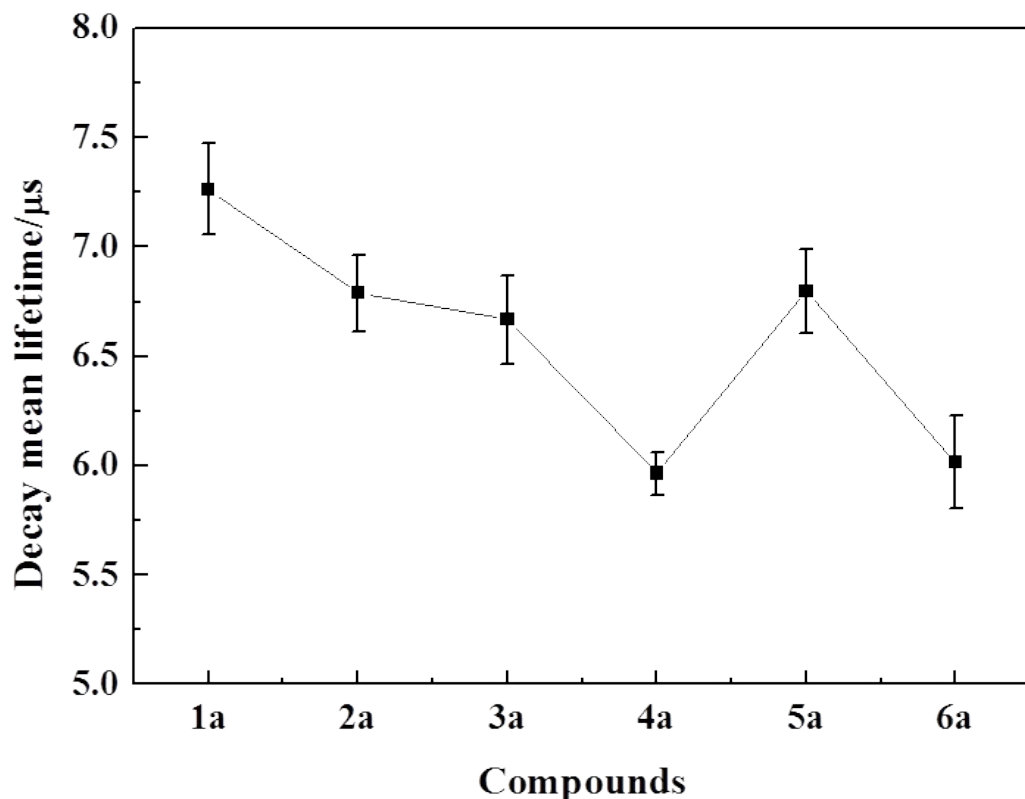


Fig. S24 Error bars for the values of **1a–6a** emission lifetimes in CH_2Cl_2 at 298 K.

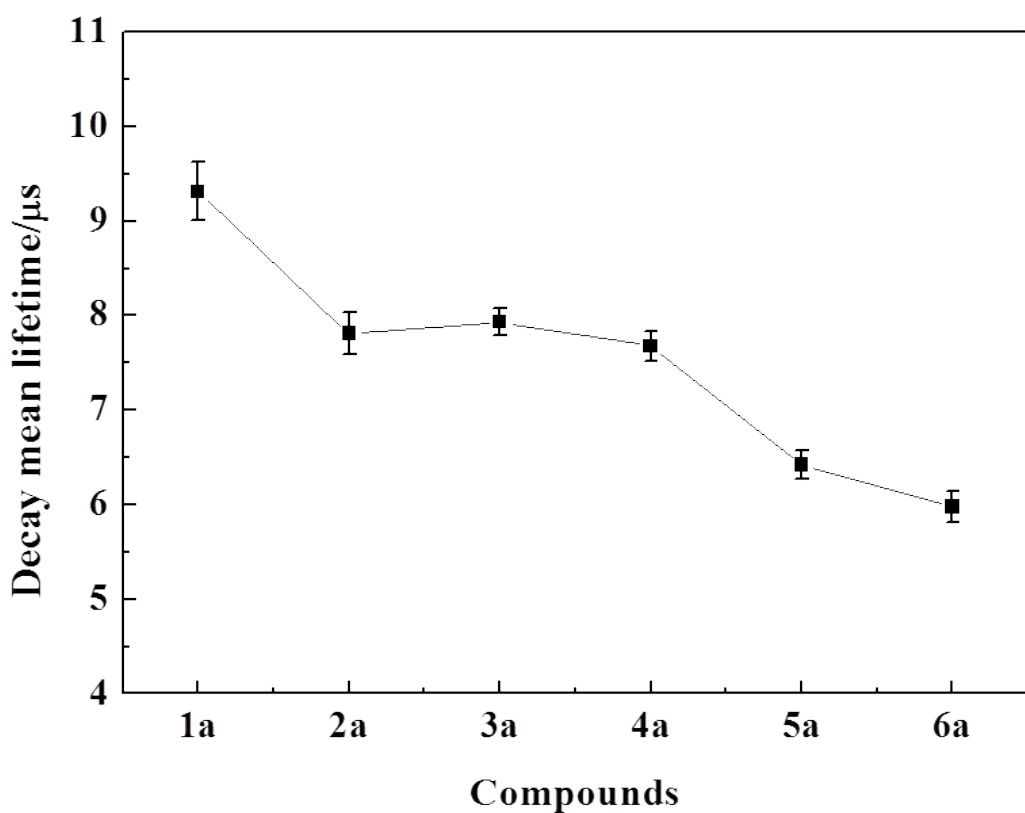


Fig. S25 Error bars for the values of **1a–6a** emission lifetimes in the solid state at 298 K.

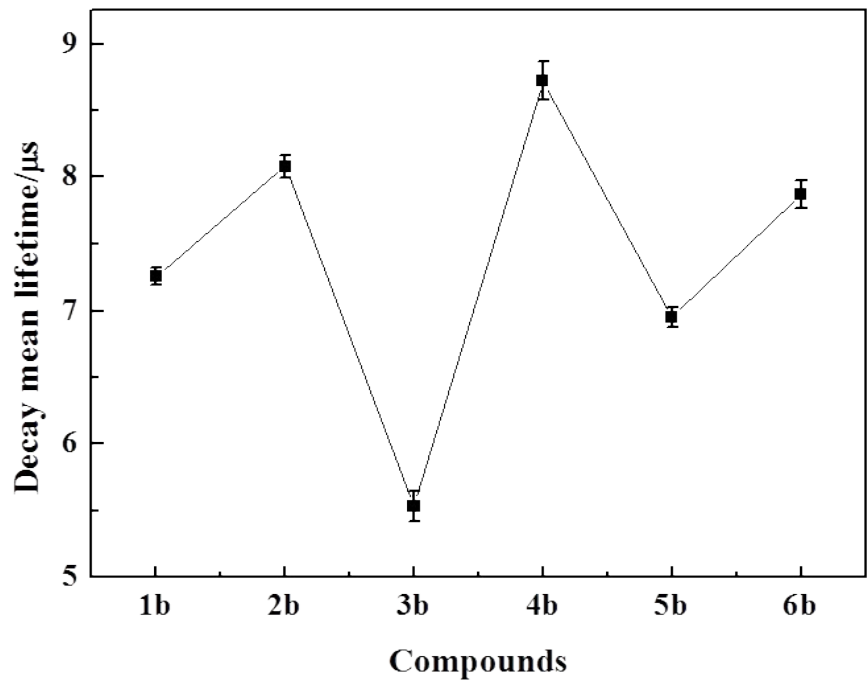


Fig. S26 Error bars for the values of **1b–6b** emission lifetimes in CH_2Cl_2 at 298 K.

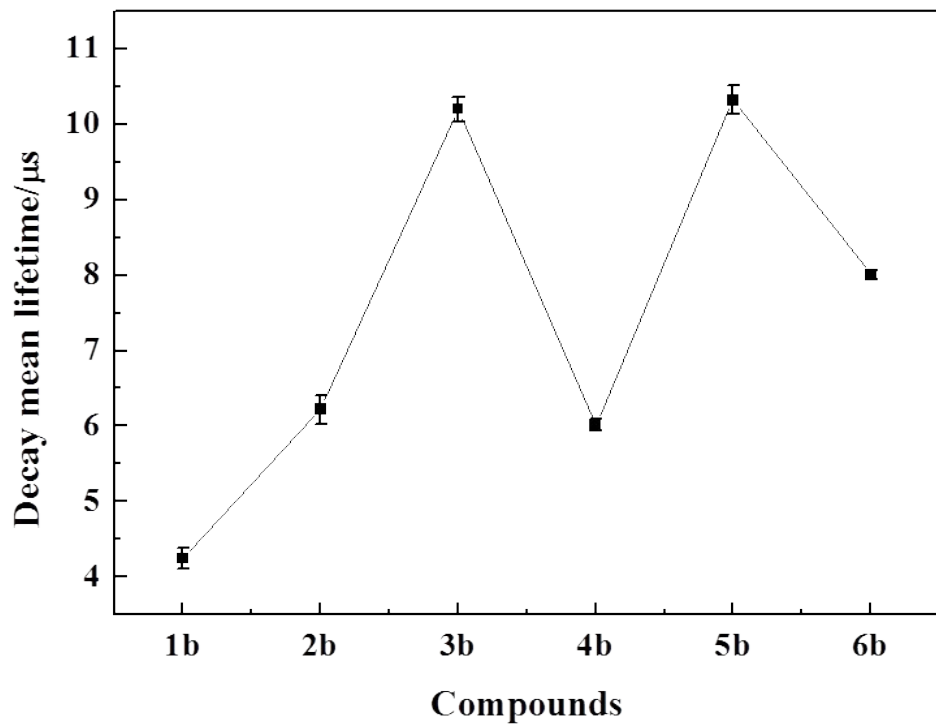


Fig. S27 Error bars for the values of **1b–6b** emission lifetimes in the solid state at 298 K.

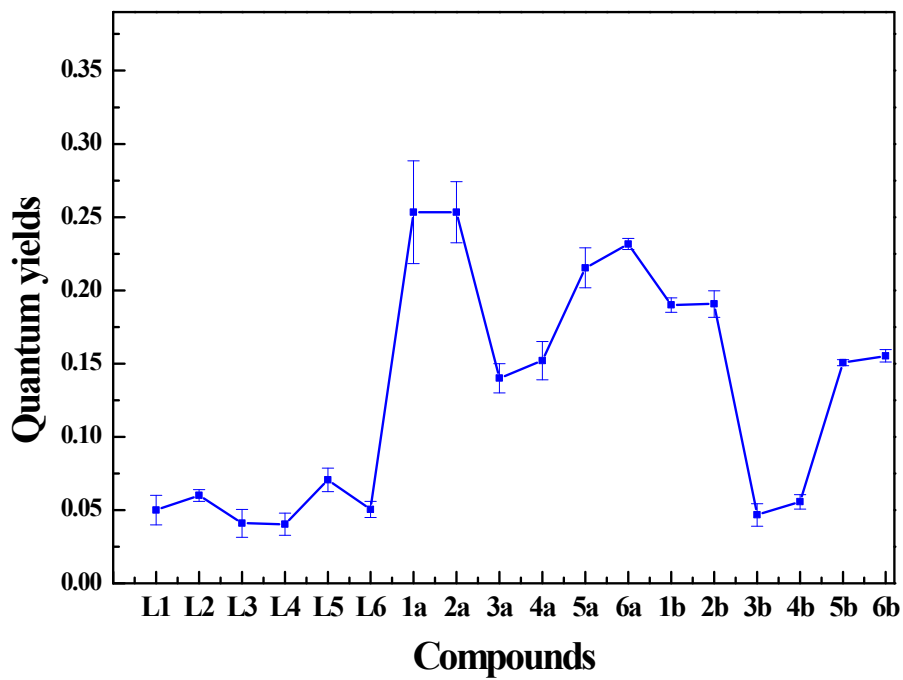


Fig. S28 Error bars for the values of **L¹–L⁶, 1a–6a, 1b–6b** Quantum yields in the CH₂Cl₂ at 298 K.

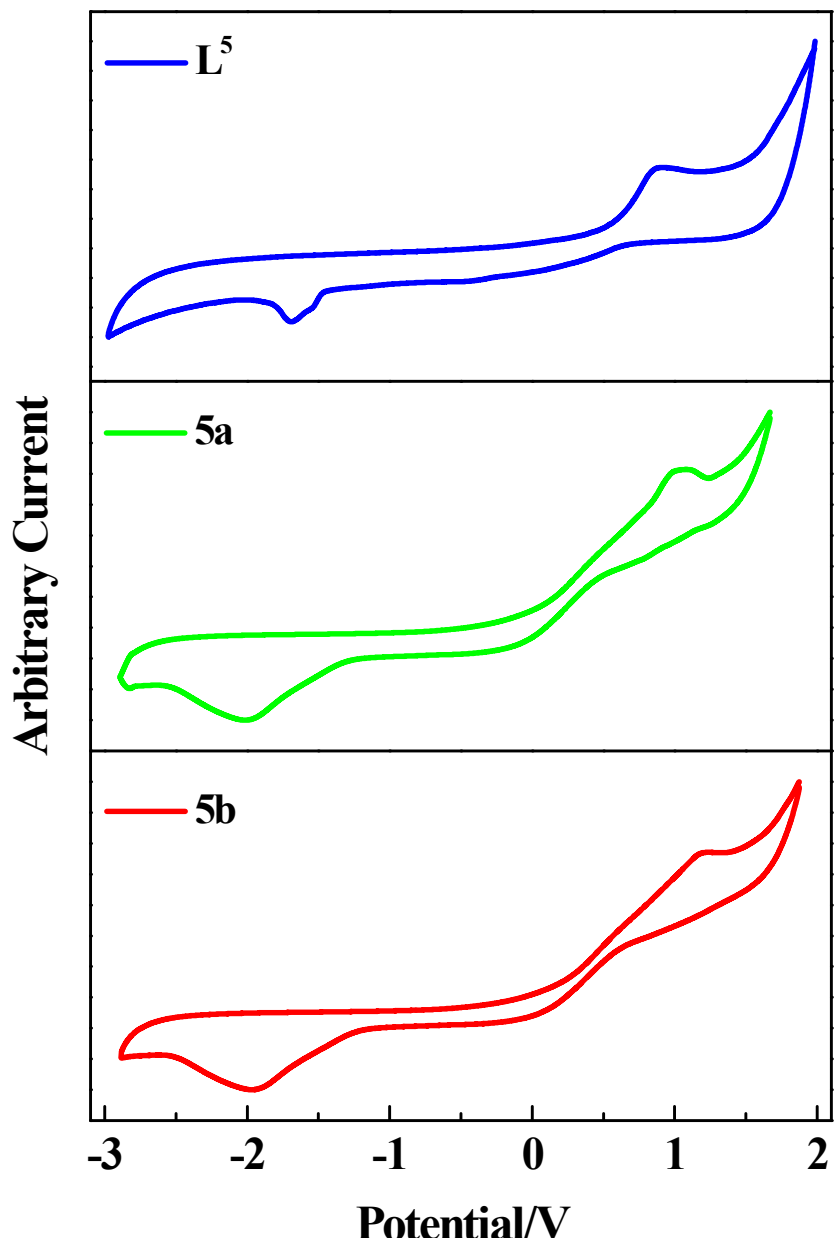


Fig. S29 Cyclic voltammograms compounds L^5 , **1a** to **1b** in CH_2Cl_2 solution (1×10^{-3} M) with 0.10 M TBAPF₆ at a scan rate of 0.10 V s⁻¹ using a glassy carbon working electrode.

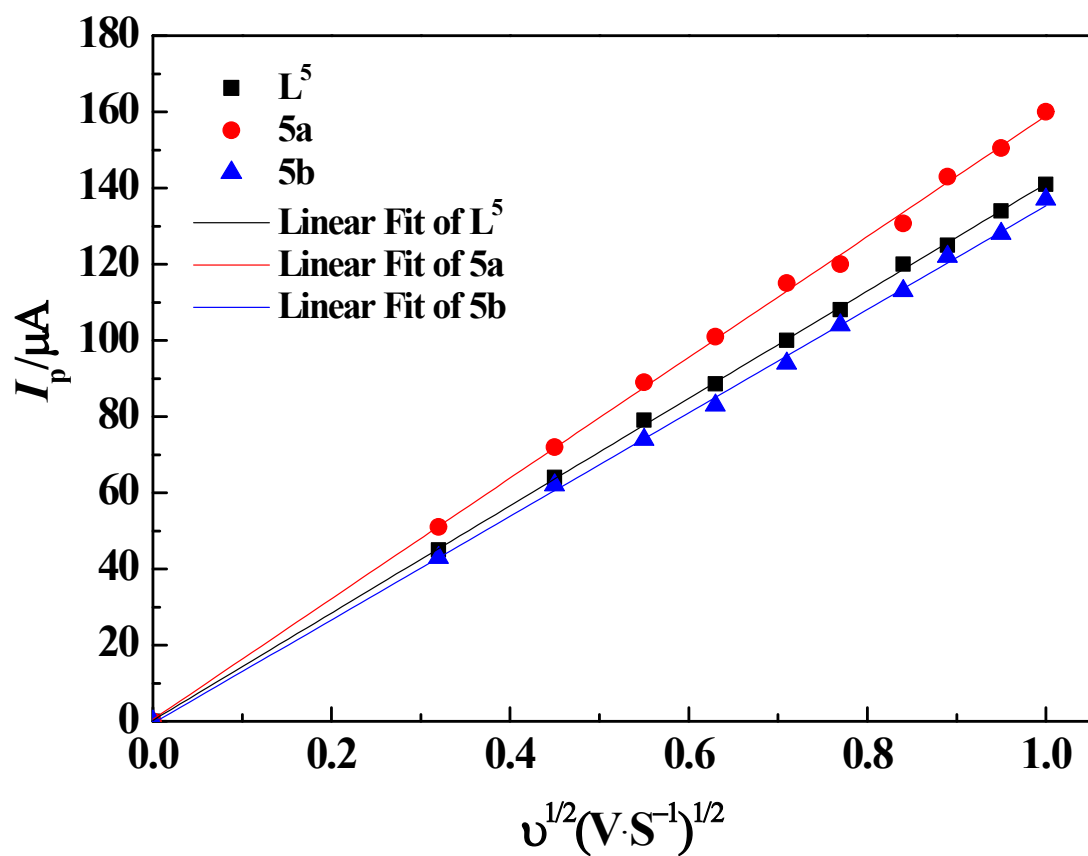


Fig. S30 The plot of $I(a,c)$ vs square root of scan rate

REFERENCES

- 1 A. Garoufis, S. Kasselouri, C. P. Raptopoulou and A. Terzis, *Polyhedron*, 1999, **18**, 585.
- 2 J. J. Lopez-Garriga, S. Hanton, G. T. Hanton, G. T. Babcock and J. F. Harrison, *J. Am. Chem. Soc.* 1986, **108**, 7251.